

**PHOTOCATALYTIC DEGRADATION AND
CHLORINATION OF AZO DYE IN SALINE
WASTEWATER**

LUK MEI KWAN

UNIVERSITI TUNKU ABDUL RAHMAN

**PHOTOCATALYTIC DEGRADATION AND CHLORINATION OF AZO
DYE IN SALINE WASTEWATER**

LUK MEI KWAN

**A project report submitted in partial fulfilment of the requirements for the
award of the degree of Bachelor of Engineering (Hons.) Environmental
Engineering**

**Faculty of Engineering and Green Technology
Universiti Tunku Abdul Rahman**

September 2016

DECLARATION

I hereby declare this project report is based on my original work except for citations and quotations which have been duly acknowledged. I also declare that it has not been previously and concurrently submitted for any other degree or award at UTAR or other institutions.

Signature : _____

Name : _____

ID No. : _____

Date : _____

APPROVAL FOR SUBMISSION

I certify that this project report entitled **“PHOTOCATALYTIC DEGRADATION AND CHLORINATION OF AZO DYE IN SALINE WASTEWATER”** was prepared by **LUK MEI KWAN** has met the required standard for submission in partial fulfilment of the requirements for the award of Bachelor of Engineering (Hons.) Environmental Engineering at Universiti Tunku Abdul Rahman.

Approved by,

Signature : _____

Supervisor : Dr. Lam Sze Mun

Date : _____

The copyright of this report belongs to the author under the terms of the copyright Act 1987 as qualified by Intellectual Property Policy of Universiti Tunku Abdul Rahman. Due acknowledgement shall always be made of the use of any material contained in, or derived from, this report.

© 2016, Luk Mei Kwan. All right reserved.

Specially dedicated to my beloved mother.

“Thank you for your unconditional love and support in everything I do.”

ACKNOWLEDGEMENT

I would like to express my most sincere gratitude to my final year project supervisor, Dr. Lam Sze Mun for her detailed and patient guidance, invaluable advice and assistance throughout the execution of the whole project. Through this opportunity, I am grateful to have been exposed to the experience of carrying out research work under professional guidance.

My deepest gratitude also goes out to all the lab officers, Mr. Voon Kah Loon, Mr. Chin Kah Seng, Mr. Ooi Keng Fei, Ms. Ng Suk Ting, Cik Hazreena Binti Noor Izahar and Ms. Mirohsha a/p Mohan who all contributed to the successful completion of my final year project.

Furthermore, I would like to thank my friend, Christina Previtha for always being there for me. I am proud of how we have completed our respective project with each other's encouragement and endless moral support. Also, I am grateful to all my other friends who motivated me throughout my final year project as well. Most certainly, I also would like to thank my senior, Wong Kok Ann who gave me useful advices regarding my final year project work.

Last but not least, I wish to thank my mother for her love and support which helped me in doing my best to complete my final year project.

PHOTOCATALYTIC DEGRADATION AND CHLORINATION OF AZO DYE IN SALINE WASTEWATER

ABSTRACT

Textile effluents containing high amount of azo dyes and inorganic salts are largely generated and is one of the major causes of pollution due to its discharge without adequate treatment. In this study, heterogeneous photocatalysis using ZnO photocatalyst and UV-Vis light irradiation was proposed to treat the dye-containing wastewater in saline condition. The photocatalytic experiment was performed using Mordant Orange-1 (MO-1) as the model dye pollutant in the presence of Cl^- ions. ZnO photocatalyst was analyzed by XRD, FESEM-EDX and UV-Vis absorption analyses to determine its crystallinity, surface morphology with elemental composition and band gap energy, respectively. The XRD finding showed that ZnO was in hexagonal wurzite phase and the FESEM-EDX analyses exhibited that ZnO has irregular hexagonal shapes. The band gap of ZnO was determined to be 3.17 eV through the UV-Vis absorption analysis. Next, comparison study showed that ZnO has better photocatalytic activity and sedimentation ability than commercial TiO_2 . Besides, the effect of process parameters on the photocatalytic degradation of MO-1 were investigated and optimized. Under the experimental condition of 200 mM salinity concentration, 2.5 mg/L initial MO-1 concentration and solution pH 5.6, photocatalytic degradation efficiency of MO-1 in saline condition using ZnO achieved 92.37% after 160 minutes of UV-Vis light irradiation. In addition, mineralization study of MO-1 was investigated in terms of COD removal which achieved 67.09% after 240 minutes of light irradiation. Furthermore, kinetic study was performed employing Langmuir-Hinshelwood (L-H) first-order kinetic model. It was found that the kinetic data matched well with the L-H first-order model with the values k_{L-H} and K obtained equal to 0.1726 mg/L•min and 0.0336 L/min.

TABLE OF CONTENTS

DECLARATION	ii
APPROVAL FOR SUBMISSION	iii
ACKNOWLEDGEMENT	vi
ABSTRACT	vii
TABLE OF CONTENTS	viii
LIST OF TABLES	xi
LIST OF FIGURES	xii
LIST OF SYMBOLS / ABBREVIATIONS	xiv
LIST OF APPENDICES	xvii
CHAPTER	
1 INTRODUCTION	1
1.1 Textile Industry and Advanced Oxidation Processes in Saline Wastewater Treatment	1
1.2 Problem Statements	3
1.3 Research Objectives	4
1.4 Scope of Study	5
2 LITERATURE REVIEW	6
2.1 Azo Dyes in Saline Wastewater	6
2.2 Methods of Dye Degradation	9
2.2.1 Physical Treatment Methods	9
2.2.2 Biological Treatment Methods	11
2.2.3 Chemical Treatment Methods	13
2.3 Advanced Oxidation Process (AOP)	13
2.3.1 Basic Principles of Heterogeneous Photocatalysis	14
2.3.2 Zinc Oxide (ZnO) as Photocatalyst	16

2.4	Parameter Studies	18
2.4.1	Salinity Concentration	18
2.4.2	Initial Concentration of Dye Solution	19
2.4.3	Solution pH	21
2.5	Kinetics of Photodegradation	22
3	RESEARCH METHODOLOGY	24
3.1	Materials and Chemicals	25
3.2	Apparatus and Equipment	25
3.3	Analytical Procedures	27
3.3.1	UV-Vis Spectrophotometer Analysis	27
3.3.2	Chemical Oxygen Demand (COD) Analysis	28
3.4	Characterization of ZnO Photocatalyst	29
3.4.1	Crystal Phase Analysis	29
3.4.2	Morphology and Elemental Analyses	29
3.4.3	Band Gap Measurement	29
3.5	Photocatalytic Activity of Photocatalyst under UV-Vis Light Irradiation	30
3.6	Operating Parameters	31
3.6.1	Salinity Concentration	31
3.6.2	Initial Dye Concentration	31
3.6.3	Solution pH	32
3.7	Kinetic Study	32
4	RESULT AND DISCUSSION	33
4.1	Characterization of ZnO Photocatalyst	33
4.1.1	XRD Analysis	34
4.1.2	FESEM-EDX Analyses	35
4.1.3	UV-Vis Absorption Analysis	38
4.2	Photocatalytic Degradation of MO-1 using ZnO under UV-Vis Light Irradiation	39
4.3	Effect of Process Parameters Studies	43
4.3.1	Effect of Salinity Concentration	43

4.3.2	Effect of Initial Dye Concentration	47
4.3.3	Effect of Solution pH	49
4.4	Mineralization of MO-1	51
4.5	Kinetic Study	53
4.5.1	Photocatalytic Degradation Kinetics of MO-1	53
4.5.2	Langmuir-Hinshelwood (L-H) Kinetic Model	55
5	CONCLUSION AND RECOMMENDATIONS	59
5.1	Conclusion	59
5.2	Recommendations	61
	REFERENCES	62
	APPENDICES	70

LIST OF TABLES

TABLE	TITLE	PAGE
2.1	Typical Characteristics of Dyes of Different Class Containing Azo Group(s)	7
2.2	General Information of MO-1	9
2.3	Dye Degradation Efficiency of Dyes at Different Salt Content	12
2.4	Effect of Solution pH on the Photocatalytic Degradation of Various Dyes	20
3.1	List of Chemicals Used in Present Study	25
4.1	The Values of k_{app} and R^2 at Different Initial MO-1 Concentrations.	54
4.2	The k_{app} values obtained in the photocatalytic degradation of dyes	55
4.3	Values of k_{L-H} and K Determined in MO-1 Degradation	58

LIST OF FIGURES

FIGURE	TITLE	PAGE
2.1	Chemical Structure of MO-1	9
2.2	Basic Mechanism of Excitation of Photocatalyst	15
2.3	The (a)rocksalt, (b)zinc blende, (c)wurzite ZnO crystal structures	17
3.1	Flow Chart of Experimental Procedures of This Study	24
3.2	Photocatalytic System	26
3.3	Schematic Diagram of Photocatalytic System	27
3.4	<i>Hach DRB 200</i> COD Digestor Reactor	28
4.1	XRD Spectrum of Commercial ZnO Powder	34
4.2	FESEM Image of ZnO Powder at magnification of: (a) 30,000x, (b) 80,000x	35
4.3	EDX Spectrum of ZnO Powder	36
4.4	EDX Spectrum of ZnO Sample Treated at Different Salinity Concentration: (a) 50 mM, (b) 200 mM, (c) 800 mM	37
4.5	UV-Vis Absorption Spectrum of ZnO photocatalyst	38
4.6	UV-Vis Absorption Spectra of MO-1 Dye Contained 200 mM Cl ⁻ Solution Using UV-Vis/ZnO at Different Time Intervals and (b): The Colour Change of MO-1 Dye Contained 200 mM Cl ⁻ Solution Using UV-Vis/ZnO at Different Time Intervals ([MO-1] = 5 mg/L; ZnO loading = 1.0 g/L; Solution pH = 5.6)	40

4.7	Photocatalytic experiment of MO-1 Degradation Contained 200 mM Cl ⁻ using photolysis, dark/ZnO, UV-Vis/ ZnO and UV-Vis/TiO ₂ ([MO-1] = 5 mg/L; Photocatalyst loading = 1.0 g/L; Solution pH = 5.6)	41
4.8	Sedimentation for 30 min in MO-1 Solution After UV-Vis Light Irradiation: (a) ZnO and (b) TiO ₂ photocatalyst	43
4.9	Effect of Salinity Concentration on MO-1 Degradation Using ZnO Photocatalyst ([MO-1]= 5 mg/L; ZnO Loading = 1 g/L; Solution pH = 5.6)	44
4.10	Proposed Degradation Mechanism of ZnO Photocatalyst in The Presence of Cl ⁻ ions	45
4.11	Effect of Initial Dye Concentration on MO-1 Degradation Percentage (ZnO Loading = 1.0 g/L; Salinity Concentration = 200 mM; Solution pH = 5.6)	48
4.12	Effect of Solution pH on MO-1 Degradation Percentage ([MO-1]= 2.5 mg/L; ZnO Loading = 1.0 g/L; Salinity Concentration= 200 mM)	50
4.13	Variation of MO-1 and COD Percentage Using UV-Vis/ZnO in Presence of 200 mM Cl ⁻ ions ([MO-1] = 2.5 mg/L; ZnO Loading = 1.0 g/L; Solution pH = 5.6)	52
4.14	Kinetics of Photocatalytic Degradation of MO-1 at Different Initial Dye Concentrations. (ZnO loading = 1.0 g/L; Salinity concentration = 200 mM; Solution pH = 5.6)	54
4.15	Plot of 1/r vs. 1/C of Photocatalytic Degradation of MO-1 (ZnO loading = 1g/L, Salinity concentration = 200 mM, Solution pH =5.6, t = 20 min)	57

LIST OF SYMBOLS / ABBREVIATIONS

•OH	Hydroxyl Radical
Cl ⁻	Chloride Ion
L-H	Langmuir-Hinshelwood
-N=N-	Nitrogen Double Bond Nitrogen
ZnO	Zinc Oxide
A ₀	Absorbance at $t=0$
AC	Activated Carbon
AOP	Advanced Oxidation Process
AOX	Absorbable Organic Halides
AR-88	Acid Red-88
A _t	Absorbance at a given time
A _x	Absorbance at $t=x$
BY 3G-P	Brilliant Yellow 3G-P
C	Concentration of Reactant, mg/L
C ₀	Concentration of Reactant at $t=0$, mg/L
CB	Conduction Band
C _f	Concentration at a given time
Cl	Chlorine
Cl•	Chlorine Radical
Cl ₂ • ⁻	Dichlorine Radical
CNS	Central Nervous System
CO ₂	Carbon Dioxide
COD	Chemical Oxygen Demand
COD ₀	Chemical Oxygen Demand at $t=0$
COD _f	Chemical Oxygen Demand at a given time
D _{abs}	Degree of
DO-3	Disperse Orange-3

DR-81	Direct Red-81
e^-/h^+	Electron/Hole Pair
e_{CB}	Conduction Band Electron
E_g	Band Gap Energy
eV	Electron Volt
e_{VB}	Valence Band Electron
FESEM-EDX	Field-Emission Scanning Electron Microscope coupled with Energy Disperse X-ray
h^+	Hole
H ₂ O	Water
H ₂ O ₂	Hydrogen Peroxide
HCl	Hydrochloric Acid
HO ₂ •	Hydroperoxyl Radical
HOCl• ⁻	Hypochlorine Radical
HR	High Range
$h\nu$	Photon Energy
K	Adsorption Equilibrium Constant, L/mg
k	Rate Constant
k_{app}	First-order Apparent Rate Constant (min ⁻¹)
k_{L-H}	Reaction Rate Constant, mg/L•min
MB	Methylene Blue
mM	Mili-molar
MO-1	Mordant Orange-1
n	Order of Reaction
Na ₂ SO ₄	Sodium Sulphate
NaCl	Sodium Chloride
NaNO ₃	Sodium Nitrate
NaOH	Sodium Hydroxide
O ₂ • ⁻	Superoxide Radical
-OH	Hydroxyl Group
PZC	Point of Zero Charge
r	Rate of Reaction
R^2	Coefficient of Linear Correlation

RB-5	Reactive Black-5
-SO ₃	Sulphonate Group
TiO ₂	Titanium Dioxide
UV-Vis	Ultraviolet-Visible
VB	Valence Band
XRD	X-ray Powder Diffraction
λ_g	Absorption Edge, nm

LIST OF APPENDICES

APPENDIX	TITLE	PAGE
A	Mordant Orange-1 (MO-1) Calibration Curve	70
B	Mordant Orange-1 (MO-1) UV-Vis Absorption Spectrum	71

CHAPTER 1

INTRODUCTION

1.1 Textile Industry and Advanced Oxidation Processes in Saline Wastewater Treatment

Synthetic dyes are extensively used in industries such as textiles, cosmetics, plastics and food which in turn generate large amount of dye-containing wastewater (Jeyasubramanian, Hikku & Sharma, 2015; Yamjala, et al., 2015). It was reported that textile industry is the largest consumer of synthetic dyes and the principal generator of dye-containing wastewater (Tan, et al, 2015; Arora, 2014; Ratna & Padhi, 2012). It was estimated that 2% of dyes are lost to the wastewater stream during dye production stage and a loss of 15% during dyeing processes due to incomplete binding to fabrics (Tan, et al, 2015; Arora, 2014). The estimated yearly loss of dyes from textile industry is up to 200,000 tons (Chequer, et al., 2013).

In addition, textile effluent was also characterized by high salt content besides its high dye content (Yuan, et al., 2012; Yu, et al., 2015). Sodium salts such as sodium chloride (NaCl), sodium sulphate (Na₂SO₄) and sodium nitrate (NaNO₃) are dyeing additives added to improve the adsorption of dye particles onto fabrics (Khalid, et al., 2012; Aleboyeh, et al., 2012). Among the salts used, NaCl is the most common salt used due to its lower cost (Yuan, et al., 2012). Intense concern has been raised over the pollution caused by textile effluents which are discharged without effective and adequate treatment (Yao, et al., 2016).

Among the synthetic dyes, azo dyes are the largest group of dyes used in the industries which rendered them the main constituent in textile effluents. Azo dyes have complex and refractory structures that can bring deleterious effects to the environment especially aquatic ecosystems and human health (Hung, et al., 2012; Arora, 2014). In fact, azo dyes and their breakdown products such as benzidine and amines are well reported to be toxic, carcinogenic, neurotoxic and genotoxic by Hung, et al. (2012) and Yamjala, et al. (2015). Furthermore, salts discharged through textile effluent can bring adverse environmental impacts as well. Salts increase salinity of water and soil which in turn adversely affect growth of aquatic organisms and plants (Mobar, Kaushik & Bhatnagar, 2015). In addition, salt anions such as chloride (Cl^-) ions can react with dye compounds to generate harmful chlorinated compounds that possessed toxicity and carcinogenicity characteristics (Yuan, et al., 2012; Vacchi, et al., 2013).

Conventional wastewater treatment methods including physical, chemical and biological methods are utilized in treating saline textile effluent (Singh & Arora, 2011; Ratna & Padhi, 2012). These methods have been widely reviewed and found to have varied level of success and showed drawbacks such as production of sludge and residue that caused disposal concern in methods such as coagulation-flocculation, membrane filtrations and biological treatments (Ratna & Padhi, 2012; Karthik, et al., 2014) and secondary pollution caused by chemicals used in chemical treatment methods (Karthik, et al., 2014). Besides, presence of salts in textile effluent can affect treatment efficiency as well. Yuan, et al. (2012) and Dindarloo, et al. (2015) reported that, certain biological methods are ineffective in treating saline wastewater due to the inability of the bacteria in withstanding high salinity environment where they underwent plasmolysis. In addition, one critical limitations faced by conventional methods are the incapability to completely degrade dye compounds into benign substances and the partially degraded compounds still remain as a threat (Priyanka & Srivastava, 2013; Karthik, et al., 2014).

A favourable alternative to conventional treatment methods known as Advanced Oxidation Process (AOP) and it has been widely applied in treating textile wastewater owing to its effectiveness in treating dye-containing wastewater (Singh & Arora, 2011; Karthik, et al., 2014). Among AOPs, Heterogeneous photocatalytic

degradation is one of the promising technologies and has shown possibility in degrading dye compounds completely into harmless compounds such as Carbon Dioxide (CO₂), water (H₂O) and organic acids (Priyanka & Srivastava, 2013).

1.2 Problem Statements

Azo dyes are well documented to be persistent to degradation due to its complex aromatic structures and are released into the water bodies through industrial effluents (Arora, 2014; Dalvand, et al., 2015). Azo dyes can be reduced in anaerobic condition as well for example in the sediments of the water bodies and breakdown into amines, benzidine and other aromatic compounds which are toxic, carcinogenic, neurotoxic and genotoxic (Hung, et al., 2012; Yamjala, et al., 2015) thus endangering the aquatic ecosystem and human health with possible health disorders such as kidney, reproductive system, liver, brain and Central Nervous System (CNS) damage; and ulceration of skin and mucous membranes (Hung, et al., 2012). Further challenges are faced as textile effluent also contains high amount of NaCl which can generate chlorinated aromatic by-products which are potentially as dangerous as the dyes and dye intermediates (Hung, et al., 2012; Yuan, et al., 2012).

Various conventional treatment techniques including physical, biological and chemical methods have been used to treat dye wastewaters. These methods have been reported with varying degrees of success (Ratna & Padhi, 2012; Karthik, et al., 2014). In recent years, AOP has shown promising results with possibilities in completely mineralizing dye compounds into harmless substances (Priyanka & Srivastava, 2013; Karthik, et al., 2014). Heterogeneous photocatalytic degradation is one of the AOPs that showed encouraging outcomes in complete degradation of wide ranges of organic pollutants including azo dyes (Lam, et al., 2012). The principle of heterogeneous photocatalysis involves an insoluble semiconductor as catalyst which can initiate a series of reactions that involves generation of free radicals and destruction of target pollutant after being irradiated sufficiently by a suitable light source. This is an environmental friendly process to treat dye-containing wastewater.

Titanium Dioxide (TiO_2) is the most widely used semiconductor in heterogeneous photocatalysis owing to its exceptional photoactivity, availability and also it is inert and corrosion resistant (Coronado, et al., 2013; Lam, et al., 2012). Zinc Oxide (ZnO) is another type of semiconductor which has showed comparable potential as an alternative for TiO_2 where ZnO has good stability, low cost and has been revealed to have higher photocatalytic activities than TiO_2 (Muthirulan, Meenakshisundararam & Kannan, 2012; Lam et al., 2012) and has favourable band gap energy (about 3.2 eV) similar to TiO_2 . In light of the encouraging trend shown by ZnO catalyst, it is employed in this study to determine its efficiency in azo dyes degradation and mineralization.

1.3 Research Objectives

The specific objectives of the present study are:

1. To characterize ZnO photocatalyst using X-ray power Diffraction (XRD), Field-Emission Scanning Electron Microscopy with Energy Disperse X-ray (FESEM-EDX) and UV-Vis absorption analyses.
2. To examine the effect of operating parameters such as salinity concentration, initial dye concentration and solution pH on Mordant Orange-1 (MO-1) degradation efficiency using ZnO under UV-Vis light irradiation.
3. To study the reaction kinetic parameters of MO-1 degradation based on a Langmuir-Hinshelwood (L-H) first-order kinetic model.

1.4 Scope of Study

In the present study, photocatalytic degradation and mineralization efficiencies of azo dye, Mordant Orange-1 (MO-1) using ZnO photocatalyst will be studied under UV-Vis light irradiation. Characterization of ZnO photocatalyst will be examined through the XRD, FESEM-EDX, and UV-Vis absorption analyses.

The performance of ZnO photocatalyst will then be evaluated with different operating parameters. This study will be carried out by varying operating parameters such as solution pH (pH 3-10), salinity (50-800 mM NaCl) and initial dye concentration (2.5-20.0 mg/L). Concentration of dye solution before and throughout the photocatalysis process will be determined using UV-Vis spectrophotometer. The operating parameters that yield the highest dye degradation efficiency will be determined and followed by the mineralization study. Subsequently, the results will be employed for kinetic study based on L-H kinetic model.

CHAPTER 2

LITERATURE REVIEW

2.1 Azo Dyes in Saline Wastewater

Azo dyes are the largest group of synthetic dyes applied in various industries such as textiles, cosmetics, plastics, food and so on (Dalvand, et al., 2016). It has been reported that azo dyes constituted 60-70% of the 100,000 commercial dyes available hitherto (Balapure, et al., 2014; Tan, et al., 2015). Textile industry was reported to be the major generator of dye-containing effluent among all industries. The effluent was commonly characterized by high organic dye content and high salt content (Ratna & Padhi, 2012; Yuan, et al., 2012). Azo dyes enter the wastewater stream during dye manufacturing processes as well as through the effluents from the mentioned industries. The estimated dye losses during the production stage and dyeing processes were 2% and 15% respectively (Tan, et al, 2015; Arora, 2014). During the dyeing processes, dye losses to the wastewater stream are consequence of incomplete binding of dyes to fabrics (Tan, et al, 2015; Arora, 2014).

Azo dyes are aromatic compounds that consists of one or more azo groups (-N=N-) with its aromatic ring mostly substituted by a sulfonate group (SO₃), hydroxyl group (OH) or amino group (Priyanka & Srivastava, 2012; Yamjala, et al., 2015; Sharma & Sanghi, 2012). Common dye classes that contain azo groups are Acid, Basic, Direct, Disperse and Reactive dyes. The characteristics of the mentioned dyes are summarized and exhibited in Table 2.1.

Table 2.1: Typical Characteristics of Dyes of Different Class Containing Azo Group(s) (Campos Ventura-Camargo & Marin-Morales, 2013; Lam, et al.,2012; Kent, 2012).

Dye class	Descriptions	Examples of dyes
Acid	Anionic dyes, water soluble, consists of one or more sulphonic or carboxylic groups in their molecule.	Acid Balck-1, Acid Blue-25
Basic	Cationic dyes, water-soluble.	Basic Blue-22, Basic Red-18
Direct	Anionic dyes, water-soluble, increased affinity to fibres in presence of electrolytes.	Direct Red-81, Direct Yellow-28
Disperse	Nonionic dyes, insoluble in water.	Disperse Yellow-42, Disperse Orange-13
Reactive	Cationic dyes with simple structures.	Reactive Black-5, Reactive Blue-19
Mordant	Anionic dyes that resemble non-metalized acid dyes.	Mordant Orange-1, Mordant Black-11

In addition, sodium salts such as NaCl, Na₂SO₄ and NaNO₃ were added as dyeing auxiliaries to improve dye adsorption onto fabrics in textile industries (Yuan, et al., 2012; Dridi-Dhaouadi & Mhenni, 2014). These salts contributed to the salinity of textile effluent. Salinity refers to the salt content of the effluent. Among all the salts used, NaCl was the most common salt used which has a lower cost (Yuan, et al., 2012).

Ineffective treatment of the azo dye in saline wastewater prior to discharge into water bodies have given rise to negative environmental impacts particularly on aquatic ecosystem and human health (Hung, et al., 2012; Arora, 2014). Discharge of azo dyes into water bodies without treatment can cause colouration of water surfaces which in turn reduces light penetration into the water bodies that can significantly reduce photosynthetic activity causing lacking of oxygen within the water body

(Karthik et al., 2014). Oxygen deficiency can adversely affect growth of aquatic lives (Malik & Grohmann, 2012).

Apart from their colours, azo dyes have been reported to have complex and recalcitrant structures which were difficult to be completely degraded into harmless substances (Arora, 2014). Moreover, azo dyes can be partially degraded in the environment into their intermediates such as which were well reported to be toxic, carcinogenic, neurotoxic and genotoxic than parent dye compounds. Reduction of azo dyes in aquatic bodies resulted in generation of dye intermediates which were aromatic compounds such as amines and benzidine that jeopardized lives of aquatic organisms due to their toxicity (Zaharia & Suteu, 2012; Hung, et al., 2012).

Discharged salts can bring adverse impacts to the environment as well such as increasing the salinity of water bodies and soil due to salt percolation and can inhibit the growth of plants (Mobar, Kaushik & Bhatnagar, 2015). Saline wastewater can also cause ineffective degradation of azo dyes in treatment processes. For instance, certain bacteria or other microorganisms are unable to withstand high salinity environment where their cells will be plasmolyzed and hence causing ineffective treatment of the dye-containing wastewater (Dindarloo, et al., 2015). Furthermore, chloride ions (Cl^-) present in NaCl salt can form undesired chlorinated compounds with dye intermediates during treatment processes of textile effluent. The chlorinated compounds were reported to be potentially carcinogenic and some even more dangerous than their parent compound (Vacchi, et al., 2013; Yuan, et al., 2012).

In present study, Mordant-Orange-1 (MO-1) azo dye as depicted in Figure 2.1 was used as a model pollutant for ZnO mediated photocatalytic degradation under UV-Vis light irradiation. General information of MO-1 is summarized in Table 2.2.

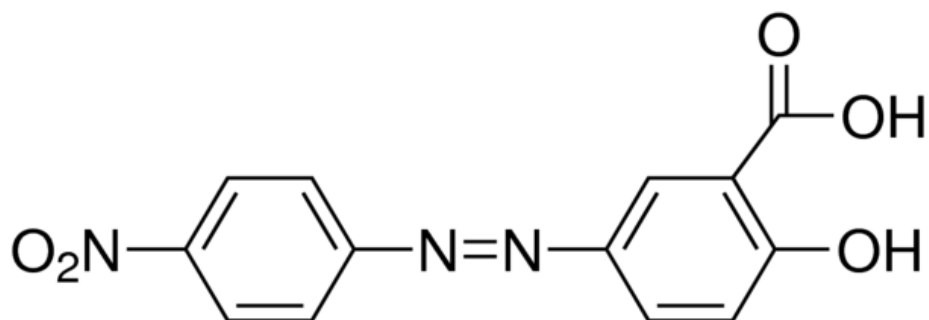


Figure 2.1: Chemical Structure of MO-1 (Sigma-Aldrich, 2016).

Table 2.2: General Information of MO-1 (Sigma-Aldrich, 2016).

Characteristics	Mordant Orange-1
Alternate name	5-(4-Nitrophenylazo)salicylic acid, Alizarin Yellow R
Colour index (CI)	14030
Chemical Formula	$C_{13}H_9N_3O_5$
Molecular weight	287.23 g/mol
Wavelength (λ_{max})	385 nm
Dye class	Mordant

2.2 Methods of Dye Degradation

Conventional treatment methods have been employed in treating azo dye in saline condition, which includes physical, biological and chemical methods (Singh & Arora., 2012; Karthik, et al., 2014). Each of the treatment method exhibits distinct efficiency and shortcomings in their application in dye degradation. These treatment methods will be discussed in the following sections.

2.2.1 Physical Treatment Methods

Physical treatment method also known as mechanical treatment method, involves only physical processes without transforming the pollutants present in the wastewater chemically (Koprivanac & Kusic, 2009). Physical treatment methods such as adsorption, coagulation-flocculation have been commonly used to remove dye from dye-containing wastewater (Koprivanac & Kusic, 2009; Singh & Arora., 2012; Karthik, et al., 2014).

Adsorption using activated carbon (AC) is the most common type of adsorption used to remove dye from wastewater and AC has been widely studied and reported to be a good adsorbent (Mezohegyi, et al., 2012). Activated carbon can be derived from organic materials such as coal, wood and other biomasses which commercial AC is derived from coal. Dagdelen, et al. (2014) have shown effective Remazol Brilliant Blue R degradation using commercial AC with the degradation efficiency of 199.45 mg/g. Other alternate and low-cost AC derived from natural sources such as saw dust, rice husk and so on was also employed in removing dye from wastewater (Hung, et al., 2012). In a study carried out by Aadil Abbas, et al., (2012), degradation of Congo red and brilliant green are studied using activated carbon derived from peanut shell as the adsorbent. Degradation efficiency of Congo red was 15.09 mg/g and that of brilliant green 19.92 mg/g and has shown possibilities in employing other adsorbents alternate to activated carbon. However, adsorption method is not preferred as the toxicity of dyes is not reduced by breaking it down but merely removing it from the wastewater and become pollution in another form (Karthik, et al., 2014).

Coagulation-flocculation utilizes coagulants such as aluminium or iron salts to enable dye particles to agglomerate and form huge particles which can be removed. This method was considered as physical method even when chemical was applied was due to the fact that dyes do not transform chemically during this process which led to a problem for the disposal of the flocs which were still toxic (Ratna & Padhi, 2012).

2.2.2 Biological Treatment Methods

Biological treatment methods utilize microorganisms in their processes to degrade pollutants in wastewater. Biological treatment techniques including microbial degradation and adsorption using living or dead microbial biomass were applied in treating dye-containing wastewater where the former was more common and widely applied in current technologies, as well as conventional wastewater treatment (Hung, et al., 2012). Biodegradation of dyes can be carried out in both aerobic and anaerobic condition. Activated sludge is one of the most typical biological methods employed to treat wastewater in aerobic condition but was found to be ineffective in dye degradation owing to the fact that most dyes are not readily degradable in aerobic condition. In Mohanty, Dafale & Rao's (2006) study, they have shown low dye (Reactive Black-5) degradation of 7% in presence of oxygen (3 mg/L) by a mixture of microorganism. In contrast, the degradation efficiency reaches maximum when amount of oxygen is reduced to 0.5 mg/L. Mohanty, Dafale & Rao (2006) have reported that optimal dye degradation occurs in anaerobic condition followed by aerobic treatment.

Biodegradation of azo dyes in anaerobic/aerobic condition takes place in a manner where anaerobic reduction of azo bond occur producing amines which are subsequently degraded aerobically leading to possible complete mineralization (Sarayu & Sandhya, 2012). Despite the successful discovery of the importance of the anaerobic phase in degrading azo dyes, biodegradation still faces limitations in terms of suitable microorganisms that can be widely applied and completely mineralization of refractory dye compounds.

In terms of growth substrate, only certain microorganisms can metabolize dyes and utilize it as their energy source. In contrast, an organic carbon source such as glucose has to be provided for microorganisms that are unable to use dyes as their growth substrate. In addition to this, microorganisms are also selectively on the types of dyes which they are able to metabolize. Blumel, Busse & Kampfer (2001) have demonstrated that *Xenophilus azovorans* KF46 can degrade carboxy-Orange I and use the dye itself as the exclusive carbon source, however when the dye is replaced by analogues sulfonated dyes, the named bacteria could not use sulphonated dyes as

energy source. This has clearly shown the difficulty in sourcing for suitable microorganisms that has the ability to metabolize broad varieties of dyes.

Many microorganisms are also sensitive to saline environment where high amounts of salts are present in dye-containing wastewater (Khalid, Arshad & Crowley, 2008). Khalid, Arshad & Crowley (2008) therefore utilized salt-tolerant *Sherwanella putrefaciens* AS96 in their studies and have obtained significant dye degradation of four structurally distinct azo dyes namely Acid Red 88 (AR-88), Reactive Black 5 (RB-5), Direct Red 81 (DR-81) and Disperse Orange 3 (DO-3). The results obtained in their studies are summarized in Table 2.3.

Table 2.3: Dye Degradation Efficiency of Dyes at Different Salt Content (Khalid, Arshad & Crowley, 2008).

Dye	Salt content (mg/L)	Dye degradation efficiency (%)	Time taken (h)
AR-88	50	100	24
RB-5	0-30	61-80	2
	40-50	100	8
	60	100	24
DR-81	40	100	8
	50	87	12
		100	20
DO-3	50	100	12

The results have showed that growth of bacteria were inhibited at high salt content and therefore consumed much longer time in reaching complete dye degradation the four dyes under study. This has also evidently showed that only limited types of microorganisms are capable of withstanding saline condition which is another limitation of application of biological method in treating azo dyes.

2.2.3 Chemical Treatment Methods

Conventional chemical oxidation method using strong oxidants such as chlorine and ozone gases is the most common chemical treatment employed to remove colour from dye-containing wastewater (Hung, et al., 2012; Karthik, et al., 2014). Chlorination has shown desirable outcome in removing colour in wastewater but have faced limitation in mineralizing toxic dye intermediates into benign substances. In fact, chlorination has generated harmful chlorinated organics and absorbable organic halides (AOX) with partially degraded dye compounds which are well reported to be more harmful than the original dye itself (Yuan, et al., 2012). In a study carried out by Vacchi, et al. (2013) on chlorination of an azo dye namely Disperse Red 81, *para*-chloronitobenzine was formed as a result of chlorination. The toxicity results of this formed compound were found to be more toxic than Disperse Red 81. Hence, chlorination was not satisfactory in treating azo dyes.

On the other hand, ozone became the favourable alternative to chlorine due to ozone's high reactivity towards many dye classes and no generation of chemical sludge resulted from ozonation. According to Turhan, et al. (2012) and Hung, et al. (2012), ozone was effective in treating dyes owing to its ability to directly reacting with dyes to degrade them in acidic condition, or generates reactive radicals such as hydroxyl radicals in basic condition that can subsequently react with dye molecules. Despite encouraging potential demonstrated by ozonation, it was found that only prolonged ozonation can achieve complete mineralization of dye compounds which can incur high cost as ozone was a costly oxidizing agent (Ratna & Padhi, 2012; Hung, et al., 2012).

2.3 Advanced Oxidation Process (AOP)

Advanced Oxidation Process (AOP) has been widely applied as an alternative to conventional treatment methods in treating textile wastewater owing to its effectiveness in dye degradation and mineralization (Singh & Arora, 2011; Karthik,

et al., 2014). AOPs possessed advantages as reported by Daghrir, Drogui & Robert (2013) and Gupta, et al. (2015) were:

1. Generation of highly reactive species that can react with wide ranges of organic pollutants.
2. Possible complete mineralization of organic pollutants into benign substances.
3. No residual sludge disposal/ treatment required.

Among AOPs, heterogeneous photocatalysis has shown possibility in degrading dye compounds completely into harmless compounds such as carbon dioxide (CO₂), water (H₂O) and organic acids. (Priyanka & Srivastava, 2013; Ong, et al., 2012; Akpan & Hameed, 2009).

2.3.1 Basic Principles of Heterogeneous Photocatalysis

Heterogeneous photocatalysis is a type of AOP that has shown prominent ability in degrading wide ranges of organic pollutants in wastewater including azo dyes. Heterogeneous photocatalysis utilizes a solid photocatalyst with reactions occurring at the surface of the catalyst. Solid semiconductors such as TiO₂ and ZnO are most employed as photocatalysts which are photoactive and can absorb photon energy ($h\nu$) to initiate a series of reactions which generate reactive free radicals to destruct target pollutants (Priyanka & Srivastava, 2013; Lam et al., 2012).

Semiconductors have distinct energy difference between their valence band (VB) and conduction band (CB), which is known as the band gap energy for example, TiO₂ and ZnO both have a band gap energy of 3.2eV (Daghrir, Drogui & Robert, 2013). When photons of energy higher than the band gap energy is absorbed by the photocatalyst, localized electrons at the VB (e_{VB}) will be brought to excited state and promoted to the CB and the electrons are now referred to as photo-excited electrons, e_{CB} . Simultaneously, positive holes (h^+) are formed at VB. This was known as the formation of the electron/hole (e^-/h^+) pair as shown in Eq. (2.1). Subsequently, e_{CB} and h^+ migrate separately to the surface of the photocatalyst for succeeding redox

reactions with the reactants. The basic mechanism of excitation of photocatalyst is illustrated in Figure 2.2 (Coronado, et al., 2013; Klan & Wirz, 2009; Pichat, 2013).

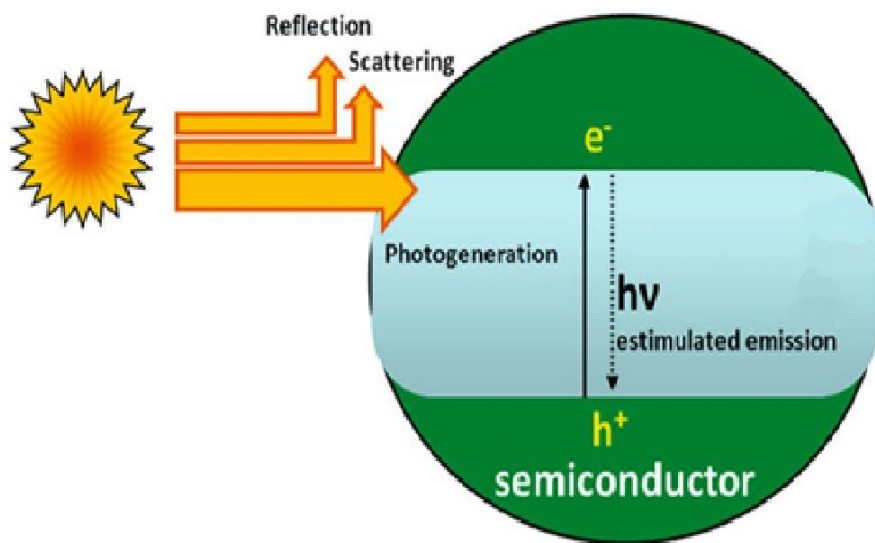
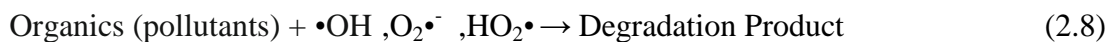
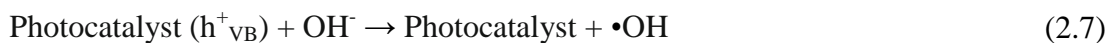
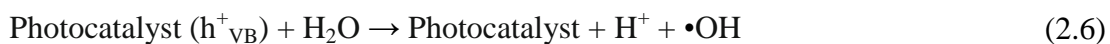
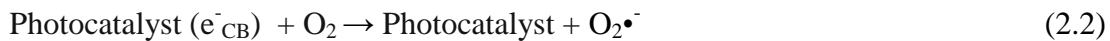


Figure 2.2: Basic Mechanism of Excitation of Photocatalyst (Coronado, et al., 2013).

Redox reactions between the (e^-/h^+) pair with the reactants occur with the presence of oxygen and can take place through two pathways which are: 1) direct electron transfer with (e^-/h^+) pair, 2) reactive radicals mediated pathway (Pichat, 2013). In the first pathway, reactants adsorbed on the surface of the photocatalyst and directly reduced/oxidized by (e^-/h^+) pair to form reduction/ oxidation products, which can be further broken down by radicals formed in the second pathway.

In contrast, the second pathway involves generation of reactive species followed by reaction with the target pollutants. O_2 molecules are first reduced by the e_{CB} into superoxide radicals ($O_2^{\bullet-}$) as shown in Eq. (2.2). $O_2^{\bullet-}$ then can be further reduced into hydrogen peroxide, H_2O_2 as shown in Eq. (2.3) which are reduced subsequently into hydroxyl radicals ($\bullet OH$), which have a high oxidizing potential of 2.8 eV as shown in Eq. (2.4). Hydroperoxyl radicals, (HO_2^{\bullet}) can be generated as well as shown in Eq. (2.5). The h^+ contributed in generating $\bullet OH$ radical as well, as shown in Eqs. (2.6) and (2.7). These generated active species then reacted with the organics to produce intermediates and eventually complete mineralization occurs as represented in Eq. (2.8). According to Sharma & Sanghi (2012), $\bullet OH$ radical is effective in degrading refractory organics due to its high reactivity and non-selectivity.

2.3.2 Zinc Oxide (ZnO) as Photocatalyst

Zinc Oxide (ZnO) is a common photocatalyst employed in heterogeneous photocatalysis next to TiO_2 . According to Di Paola, et al. (2012), ZnO has good photocatalytic properties and a wide band gap of 3.2 eV. Furthermore, ZnO has a low cost which makes it considerable in commercial applications. (Coronado, et al., 2013). ZnO has an absorption spectrum that consists of a single, broad intense absorption band of about 370 nm, which lie in the UV light wavelength range.

ZnO generally occur in three crystal structures which are rocksalt, zinc blende and wurzite structures as shown in Figure 2.3a, b and c respectively, where both rocksalt and zinc blende are cubic while wurzite is hexagonal (Johar, et al.,

2015). ZnO wurzite structure is the most common structure which exist as white hexagonal crystal (white powder) at ambient temperature and pressure and the most common form employed in photocatalysis (Lee, et al., 2016, Lam et al., 2012).

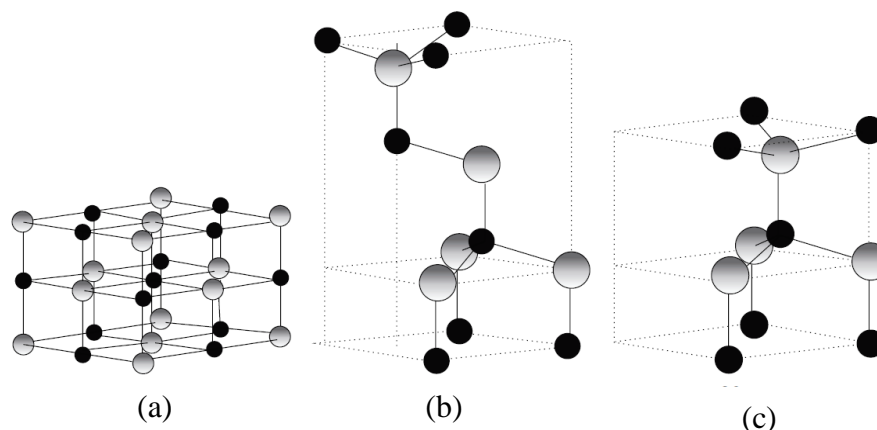


Figure 2.3: The (a) rocksalt, (b) zinc blende, (c) wurzite ZnO crystal structures (Johar, et al., 2015).

Fascinating results have been shown in many studies on ZnO photodegradation of dyes under optimized operational parameters (Lee, et al., 2016; Jia et al., 2016). ZnO catalyst was employed in a study conducted by Sobana & Swaminathan (2007) and resulted in 88% Acid Red 18 degradation under UV irradiation. Danwittayakul, et al. (2015) has shown MB degradation of 80% using ZnO composite after 180 minutes of UV irradiation time. In addition, Siuleiman, et al. (2014) has demonstrated complete Orange II degradation using ZnO photocatalyst. ZnO-based photocatalysis also shown effective degradation on other dyes such as congo red (Habibi & Rahmati, 2015), brilliant yellow 3G-P (Jia, et al., 2016), direct yellow-4 (Sobana, Krishnakumar & Swaminathan, 2013) and malachite green (Ghaedi, et al., 2014). It was therefore evident that ZnO can be applied effectively in removing recalcitrant dyes from the wastewater and to be further studied on its usage in commercial scale.

2.4 Parameter Studies

2.4.1 Salinity Concentration

Salinity refers to the salt content of the solution where it significantly affects photocatalytic degradation as reported by Konstantinou & Albanis (2004) and Muruganandham & Swaminathan (2006). The most commonly used salt in the industry was reported to be NaCl which were involved in many studies involving synthetic dyes degradation (Alventosa-deLara, et al., 2014; Yu, et al., 2015; Yuan, et al., 2012). In a study by Yuan, et al (2012), presence of Cl^- ions in NaCl salt has shown dual-effect on dye degradation where lower concentration of Cl^- enhanced dye degradation but higher concentration had the reversed effect. They found that the initial enhancement was caused by the formation of chloride radicals ($\text{Cl}\cdot$) that are good scavengers to prevent recombination of e^-/h^+ pair for effective generation of oxygen radicals for degradation of pollutants. However, increased in amount of Cl^- ions caused competition between the the mentioned ions with dyes and oxygen on the adsorption on the photocatalyst surface which led to diminished dye degradation efficiency.

Scarce studies have been conducted to study the effect of Cl^- on photocatalytic degradation of dye and this marked the importance of this present study on effect of varied concentration of Cl^- ions in degradation and mineralization of azo dyes.

2.4.2 Initial Concentration of Dye Solution

High initial concentration on dye solution has been reported to have adverse effects on dye degradation efficiency (Jia, et al., 2016; Lee, et al., 2016). Increase in dye concentration refers to the increase in amount of substrates which will be adsorbed to the photocatalyst while the number of active sites present on the catalyst

remains constant for a fixed catalyst loading, light intensity and time of irradiation. This resulted in competition between dye molecules and other molecules involved in generation of radicals such as O_2 leading to ineffective radicals generation for dye degradation and lower dye degradation efficiency.

Increased amount of dye also increases the colour intensity of the solution which leads to interception of photons before reaching the surface of catalyst. The lower light penetration causes ineffective irradiation of photocatalyst which resulted on lower dye degradation efficiency (Sangatar-Delshade, Habibi-Yangjeh & Kohahadi-Moghaddam, 2011, Lee, et al., 2016).

In Sanatgar-Delshade, Habibi-Yangjeh & Kohahadi-Moghaddam's (2011) study on the degradation of MB dye with ZnO nanoparticles, dye degradation rate has decreased from 0.1268 min^{-1} to 0.0459 min^{-1} with increasing initial concentration of MB solution from 8×10^{-6} to 2.4×10^{-6} M. In addition, Jia, et al. (2015) has found that degradation efficiency of brilliant yellow 3G-P has decreased from 95.1 to 53.1% when initial dye concentration was increased from 50 to 200mg/L after 60 minutes of irradiation time using UV-Vis light source. It is evident that increased dye concentration resulted in increased competition of molecules on adsorbing on photocatalyst surface.

2.4.3 Solution pH

Solution pH affects the surface charge of the photocatalyst thus affecting the adsorption of substrates to its surface. The studies related to influence of solution pH on dye degradation are recapitulated in Table 2.4.

Table 2.4 Effect of Solution pH on the Photocatalytic Degradation of Different Dyes.

Dye treated	Concentration (mg/L)	Time of irradiation (min)	Type of Photocatalyst	Range of pH used	Optimum pH	Degradation efficiency (%)	Reference
Congo Red	10.0	75	ZnO-CdS Nanostructure	3-9	3	88	Habibi & Rahmati, 2015
Acid Red 18		15	ZnO	3-11	11	90	Sobana & Swaminathan, 2007
Brilliant Yellow 3G-P	50.0	45	ZnO	2-12	5.1	~95	Jia, et al., 2016
MB	5.4	160	ZnO	1.5-9	9.0	~100	Sanatgar-Delshade, Habibi-Yangjeh & Kohahadi-Moghaddam, 2010
Direct Yellow-4	187.4	20	AC loaded ZnO	3-11	9.0	~95	Sobana, Krishnakumar & Swaminathan, 2013
Malachite Green	15.0	35	AC loaded ZnO	2-8	7.0	~100	Ghaedi, et al., 2014
Eriochrome Black T	25.0	20	ZnO	6-8	7.91	83	Lee, Hamid & Chin, 2015

The zero point charge pH of ZnO was reported to be about 9 by many literatures (Sanatgar-Delshade, Habibi-Yangjeh & Kohahadi-Moghaddam, 2011; Lam, et al., 2012; Sobana & Swaminathan, 2007). Surface of ZnO is positively-charged at pH below ZPC with presence of more H⁺ ions and negatively-charged at pH above ZPC by means of adsorbed OH⁻ ions (Sobana & Swaminathan, 2007).

In general, alkaline condition favours the formation of •OH as presence of more OH⁻ ions can react with photogenerated positive holes to generate more •OH for photocatalytic degradation of dyes (Akpan & Hameed, 2009). However, charges of dye particle under treatment must be taken into consideration as well. In a study conducted by Sanatgar-Delshade, Habibi-Yangjeh & Kohahadi-Moghaddam (2011), they have found that degradation of cationic dye, Methylene Blue (MB) was remarkable in ZnO mediated photocatalysis at pH above 9. At pH above 9, surface of ZnO was negatively-charged and cationic MB molecules were attracted to ZnO surface due to electrostatic attraction. On the other hand, Jia, et al. (2015) has found that degradation of anionic dye, brilliant yellow 3G-P (BY 3G-P) using ZnO photocatalyst decreased in alkaline condition due to electrostatic repulsion between negatively-charged surface of ZnO and BY 3G-P molecules.

pH of solution is also crucial in ZnO-based photocatalysis due to instability of ZnO in acidic solution. ZnO tends to dissolve by its reaction with increased amount of H⁺ ions in acidic condition as shown in Eq. (2.9) (Sanatgar-Delshade, Habibi-Yangjeh & Kohahadi-Moghaddam, 2011).



2.5 Kinetics of Photodegradation

Langmuir-Hinshelwood (L-H) model is frequently used in studying the kinetics of heterogeneous photocatalysis and was reported to be compatible with the actual experimental findings in many studies (Herrmann, 2010, Lam, et al., 2012). The rate

of degradation of reactant, r can be expressed in Eq. (2.10) where it is expressed in the units of mg/L min, C represents the concentration of reactant in mg/L, t refers to the irradiation time, k_{L-H} represents the rate constant of photocatalytic reaction in mg/L• min and K represents the adsorption constant of the reactant in L/mg (Vasanthkumar, Porkodi & Selvaganapathi, 2007).

$$r = - \frac{dC}{dt} = \frac{k_{L-H}KC}{1+KC} \quad (2.10)$$

The equation can then be simplified into linear form when C is considered as much lesser than 1 ($C \ll 1$). The simplified first order reaction is as shown in Eq (2.11) where k_{app} (min^{-1}) is the apparent first order rate constant obtained from the slope of $\ln \left(\frac{C_o}{C} \right)$ vs. t graph, C_o is the initial concentration of reactant. The theoretical data can then be computed using the simple first-order law (Asenjo, et al., 2013).

$$\ln \left(\frac{C_o}{C} \right) = k_{app} t \quad (2.11)$$

2.6 Summary

Azo dyes are the largest group of synthetic dyes applied in textile industries. Salts are used as dye additives to enhance adsorption of dyes on fabrics. Both azo dyes and salts are discharged into the environment via textile effluents. Owing to their hazardous effects, it is important to treat the azo dyes in saline wastewater adequately.

Various physical, biological and chemical methods have been employed to treat azo dyes and showed varied efficiencies in the literatures. As an alternative to these methods, AOP then emerged as a potential method that can mineralize dyes completely into innocuous substances, where heterogeneous photocatalysis was the favourable AOP that showed promising dye degradation and mineralization efficiency.

ZnO alongside with TiO₂ were the most commonly employed photocatalysts in heterogeneous photocatalysis. Photocatalytic degradation of dye was reported to be influenced by the operating parameters such as solution pH, salinity and initial dye concentration. In the photocatalytic reaction, kinetics of the photodegradation is usually compatible with a simple L-H first-order kinetic model. In this study, ZnO was selected to be used in the degradation of MO-1 azo dye in saline condition.

CHAPTER 3

RESEARCH METHODOLOGY

The experimental procedures, chemicals, materials and equipment used in present study were discussed in this chapter. The flow chart of experimental work in this study is represented in Figure 3.1.

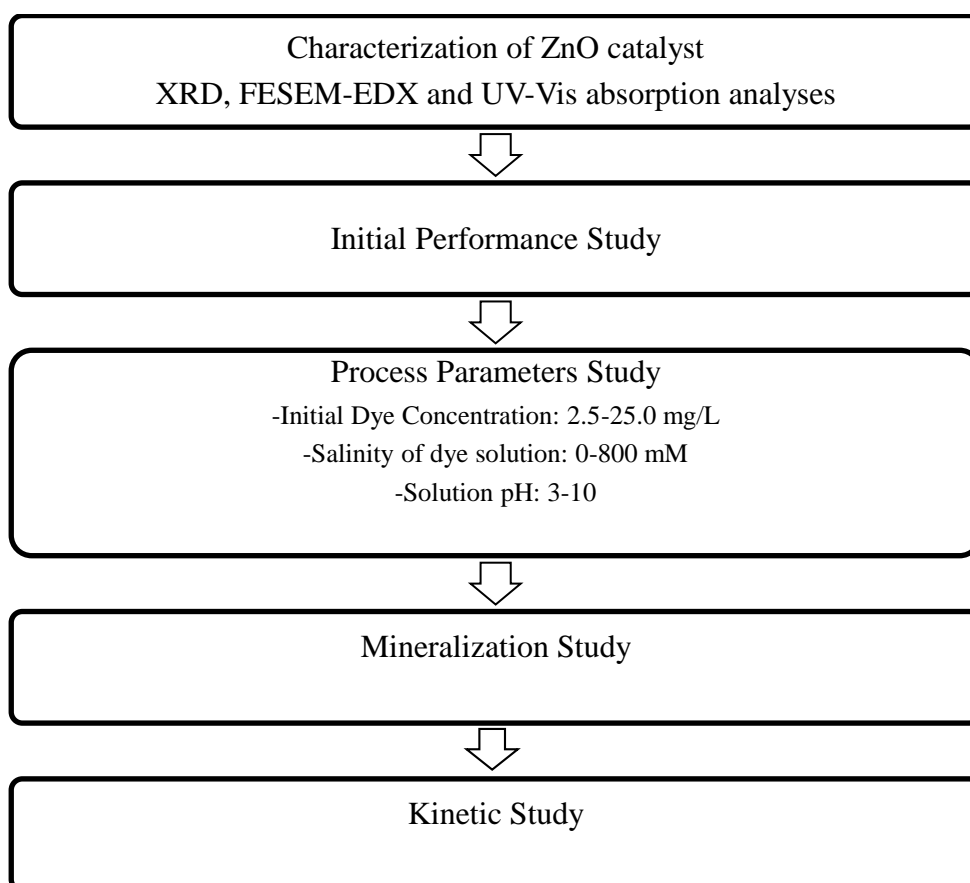


Figure 3.1: Flow Chart of Experimental Procedures of This Study.

3.1 Materials and Chemicals

All chemicals used were of analytical grade and no further purification was performed. All chemicals used in this study were shown in Table 3.1. Mordant Orange-1 (MO-1) supplied by Sigma-Aldrich Chemical Supply was employed in this study as the pollutant where solution of desired concentration was prepared by diluting concentrated MO-1 stock solution (1g/L) using distilled water (DI water) produced from Favorit water still with a resistivity of 0.3M $\Omega \cdot \text{cm}$.

Table 3.1 List of Chemicals Employed in Present Study.

Chemicals	Purity (%)	Supplier	Purpose
MO-1	70	Sigma-Aldrich Chemical Supply	Model dye
NaCl crystals	99.5	EMD Milipore	Salinity adjuster
ZnO powder	99.5	Acros Organics	Photocatalyst
TiO ₂ powder	98.0	Acros Organics	Photocatalyst
Hydrochloric acid solution (HCl)	95	Quality Reagent Chemical	pH adjuster
Sodium Hydroxide solution (NaOH)	50	Macron Fine Chemicals	pH adjuster
COD Reagent	-	Hach	COD Analysis

3.2 Apparatus and Equipment

Photocatalytic degradation of MO-1 was carried out in a photocatalytic system as shown in Figures 3.2 and 3.3. An outer black box was used as a confinement for the light generated within the apparatus and to prevent penetration of light from outside to ensure the reaction is solely mediated by the inner light source. The light source used was a 45W compact UV-Vis light with the light flux of 4100 lx (Universal

Supply Co) which was mounted on top of the black box. The apparatus also consists of a magnetic stirrer, an air pump, one inflow fan and one outflow fan. The magnetic stirrer was set to a stirring rate of 500 rpm to ensure uniform reaction of the dye solution with the photocatalyst particles. Air pump was used to provide air bubbles and the rate was adjusted using the flow meter. Air bubbles were provided at 3 L/min to aerate the photocatalytic reaction while the two fans acted as heat reducer within the reactor.

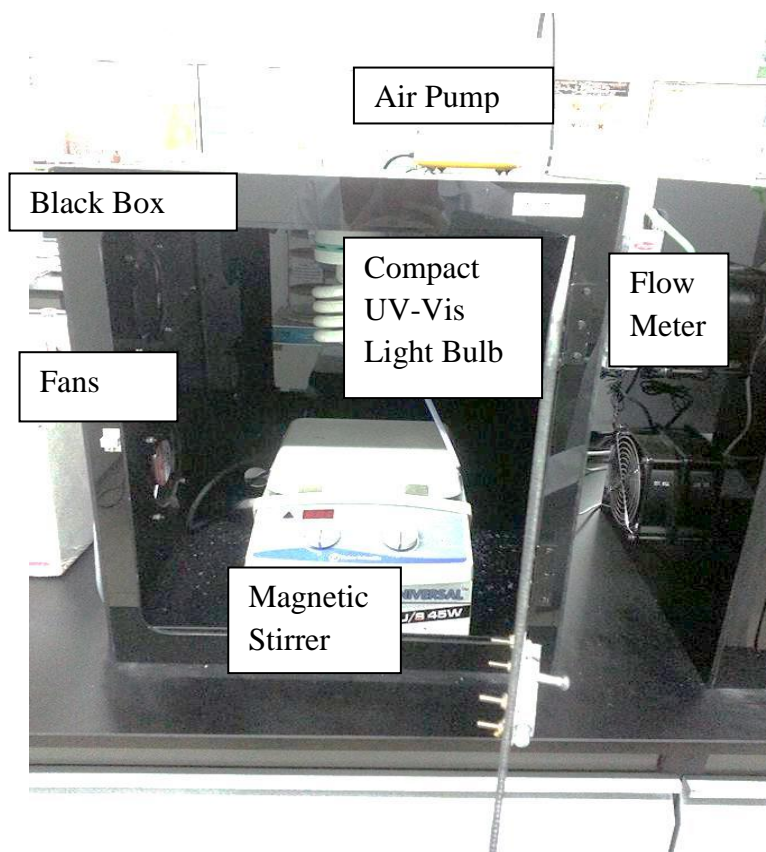


Figure 3.2: Photocatalytic System.

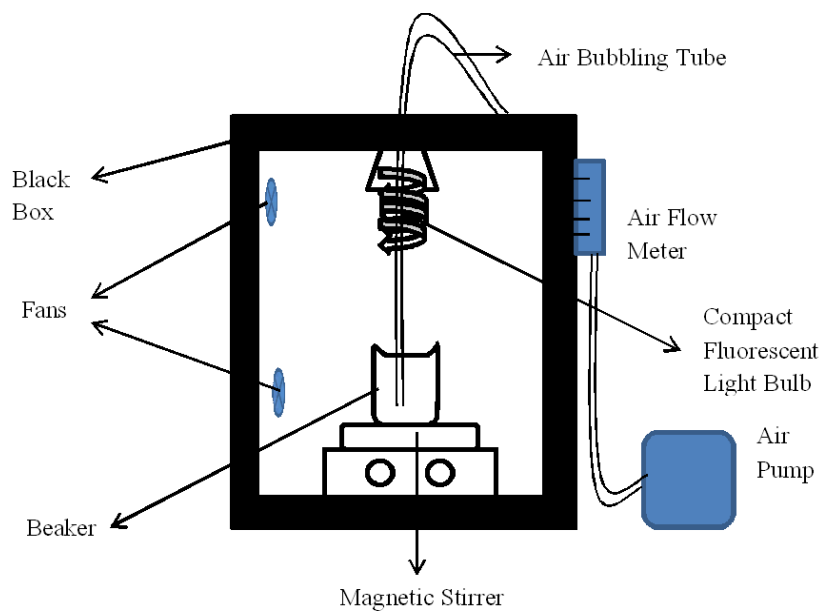


Figure 3.3: Schematic Diagram of Photocatalytic System.

3.3 Analytical Procedures

3.3.1 UV-Vis Spectrophotometer Analysis

A *Hach DR6000* UV-Vis spectrophotometer was used to generate a standard calibration curve for MO-1 and to measure the absorbance of samples of dye solution. The mode used in this spectrophotometer was the single wavelength mode where light of wavelength, $\lambda = 373$ nm was used in light of λ_{max} of MO-1.

Standard calibration curve for MO-1 was obtained by determining the absorbance values of several MO-1 standard solutions of known concentration where the spectrophotometer generated the graph of concentration, C (mg/L) versus absorbance value, A (abs). The strong linear correlation between the two parameters is represented by a correlation coefficient, R^2 of larger than 0.9.

Absorbance values of dye sample were measured and the degree of degradation of dye, D_{abs} can be computed using the A values obtained as shown in Eq. (3.1).

$$D_{\text{abs}} = \frac{(A_0 - A_t)}{(A_0 - A_x)} \times 100\% \quad (3.1)$$

Where A_0 = Initial absorbance of sample at $t=0$ minute of reaction time, abs.

A_t = Absorbance of sample at a given t minutes of reaction time, abs.

A_x = Absorbance of sample at $t=x$ minute, $A_x = 0$ was assumed, abs.

3.3.2 Chemical Oxygen Demand (COD) Analysis

A *Hach DRB 200* COD digester reactor as shown in Figure 3.4 was used to analyze the mineralization extent of dye samples. 2 mL of dye samples at different time intervals during the photocatalytic reaction was withdrawn and added into the COD high range (HR) bottle. The COD HR reagents were then placed into the COD reactor to be digested at 150 °C for 2 hours. After the 2-hour reaction, the COD samples were taken out and left to be cool at room temperature. When the COD samples have cooled down, their COD values were measured using *Hach DR6000* UV-Vis spectrophotometer.



Figure 3.4: *Hach DRB 200* COD Digester Reactor.

3.4 Characterization of ZnO Photocatalyst

3.4.1 Crystal Phase Analysis

X-ray powder diffraction (XRD) analysis was done to study the crystal phase of ZnO photocatalyst. XRD analysis was carried out using a *Philips PW 1820* diffractometer in School of Material and Mineral Resources Engineering, Universiti Sains Malaysia. Phase identification in ZnO powder performed using classical 2θ geometry using Cu- K_{α} radiation. ZnO powder produced unique diffraction pattern that differentiate it with other crystalline substances. The XRD analysis was done at Faculty of Science, Universiti Tunku Abdul Rahman (UTAR).

3.4.2 Morphology and Elemental Analyses

A *JEOL 6701-f* FESEM was used to determine the surface morphology of ZnO particles used in this study. High resolution image taken by the FESEM also provided clear determination of particle size of the ZnO powder. Prior to the analysis, ZnO sample was prepared by taping the sample on aluminium stub using a carbon tape.

EDX analysis was employed to perform elemental analysis on the photocatalyst using *JEOL 6701-f* FESEM. The elemental composition of ZnO was determined through the EDX analysis. The FESEM-EDX analyses were done at Faculty of Science, Universiti Tunku Abdul Rahman (UTAR).

3.4.3 Band Gap Measurement

UV-Vis absorption analysis was carried out in this research to estimate the band gap energy of ZnO photocatalyst. This analysis was conducted in the wavelength range of 350 to 700 nm, to study the absorption behaviour of ZnO photocatalyst at this wavelength range. The UV-Vis absorption analysis was done at School of Chemical Sciences, Universiti Sains Malaysia (USM).

3.5 Photocatalytic Activity of Photocatalyst under UV-Vis Light Irradiation

Photocatalytic activity of ZnO catalyst was studied by the degradation of MO-1 as model pollutant. 100mL sample of MO-1 solution of desired concentration was prepared in a 250mL beaker by diluting the 1g/L MO-1 stock solution. Experiment was carried out by placing the dye sample containing 1g/L of ZnO in a black box. Supply of air bubbles was given at a constant rate of 3 L/min. Dye sample was continuously mixed using a magnetic stirrer. Prior to the photocatalytic reaction under light irradiation, dark adsorption reaction in the absence of light for 1 hour was carried out. Subsequently, the sample was irradiated under UV-Vis light for 1 hour. Throughout both reactions, 5 mL of sample was withdrawn at certain time interval and centrifuged for 30 minutes. The supernatant was then filtered using a PTFE membrane syringe filter (0.45 μm pore size). Filtered sample was subsequently analyzed using spectrophotometer and COD test. The dye degradation efficiency and mineralization efficiency were calculated using Eq. (3.2) and Eq. (3.3) respectively.

$$\text{Dye degradation efficiency (\%)} = \frac{C_o - C_f}{C_o} \times 100\% \quad (3.2)$$

$$\text{Mineralization efficiency (\%)} = \frac{\text{COD}_o - \text{COD}_f}{\text{COD}_o} \times 100\% \quad (3.3)$$

where C_o is the initial concentration of the dye at $t=0$ (mg/L), C_f is the concentration at a given time (mg/L), COD_o is the initial COD value at $t=0$ (mg/L) and COD_f is COD value at a given time (mg/L).

Photocatalytic activity of TiO₂ catalyst was subsequently studied under same procedures for comparison study with ZnO.

3.6 Operating Parameters

There are many factors such as initial dye concentration, catalyst loading, salinity and solution pH that influenced the photocatalytic reaction. Three different operating parameters namely salinity concentration, initial dye concentration and solution pH were examined in this study.

3.6.1 Salinity Concentration

The effect of salinity in terms of Cl⁻ concentration (mM) on MO-1 degradation efficiency was studied by varying the salinity of dye solution at 50 mM, 100 mM, 200 mM, 400 mM and 800 mM (Yuan, et al., 2012; Rupa, et al., 2007). The experiment was carried out at dye concentration of 5 mg/L, natural dye solution pH of 5 and photocatalyst loading of 1 g/L.

3.6.2 Initial Dye Concentration

The effect of initial dye concentration on dye degradation efficiency was studied by varying the initial MO-1 concentration in dye samples prepared. The selected initial dye concentrations under study were 2.5 mg/L, 5.0 mg/L, 10.0 mg/L, 20.0 mg/L (Tiwari, et al., 2015; Abass & Raouf, 2016). The experiment was carried out at salinity of 5 g/L, natural pH of 5 and catalyst loading of 1g/L.

3.6.3 Dye Solution pH

Under optimum condition of 20 mg/L of MO-1 with salinity of 10 mg/L and 1 g/L catalyst loading, effect of dye solution pH on MO-1 degradation efficiency at pH 3, 5, 7 and 10 was studied. pH of solution was adjusted using 1.0M HCl and 1.0M NaOH. pH value was measured using a *Hanna HI 2550* multiparameters meter which was calibrated with buffer solution of pH 4, 7 and 10.

3.7 Kinetic Study

A L-H first order kinetic model was used to determine the initial degradation rate, k_{app} of MO-1 mediated by ZnO at distinct initial dye concentrations, C_o . k_{app} can be obtained from the slope of $\ln \left(\frac{C_o}{C} \right)$ vs. time, t graph as represented in Eq. (3.3) where C_o and concentration of dye solution, C were in mg/L, t in minutes and k_{app} in min^{-1} .

$$\ln \left(\frac{C_o}{C} \right) = k_{app} t \quad (3.3)$$

By determining the k_{app} at different initial dye concentrations, the optimum initial dye concentration that rendered fastest dye degradation can be determined in this study. The L-H expression in its first-order (Eq. (3.4)) can then be employed to determine the k_{L-H} , the photocatalytic reaction rate constant ($\text{mg/L}\cdot\text{min}$) and K , the adsorption equilibrium constant (L/mg) by plotting a plot $1/r$ ($\text{L}\cdot\text{min/mg}$) vs. $1/C$ (L/mg) through the relationship expressed in Eq. (3.5).

$$\ln \frac{C_o}{C} = k_{L-H} K t = k_{app} t \quad (3.4)$$

$$\frac{1}{r} = \frac{1}{k_{L-H} K C} + \frac{1}{k_{L-H}} \quad (3.5)$$

CHAPTER 4

RESULTS AND DISCUSSION

This chapter consisted of results of the present study. First section of this chapter exhibited the characterization studies of ZnO photocatalyst. The second section presented the performance of photocatalytic removal of MO-1 using ZnO at varied process parameters including salinity concentration, initial dye concentration and solution pH. Subsequently, the third section consisted of a comparison study of the performance between TiO₂ and ZnO. The fourth section described the mineralization study of ZnO photocatalyst then lastly the fifth section consisted of the kinetic study on the photocatalytic reaction based on a Langmuir-Hinshelwood (L-H) kinetic model.

4.1 Characterization of ZnO Photocatalyst

Characterization of ZnO photocatalyst was performed in this study to relate its physicochemical properties with its photocatalytic activity performance. XRD analysis was conducted to analyze the crystal phase of ZnO photocatalyst. Besides, FESEM-EDX analysis was carried out to determine the surface morphology and elemental composition of ZnO photocatalyst. UV-Vis absorption analysis was also performed to identify the region of absorption of ZnO photocatalyst.

4.1.1 XRD Analysis

Figure 4.1 illustrates the XRD spectrum of ZnO photocatalyst. As shown in the figure, main diffraction peaks were observed at the angle $2\theta = 31.82^\circ, 34.47^\circ, 36.29^\circ, 47.59^\circ, 56.65^\circ, 62.88^\circ, 66.38^\circ, 67.99^\circ$ and 69.14° , which matched strongly with the diffraction planes (100), (002), (101), (102), (110), (103), (200), (112) and (201) respectively as reported in the standard spectrum of ZnO in hexagonal wurzite phase (JCPDS No. 01-089-0510). The sharp diffraction peaks obtained indicated that the ZnO powder has high crystallinity (Bindu, et al., 2014; Yu, et al., 2012). The XRD spectrum obtained in this study was in agreement to the spectrum obtained in other literature works which verified that the ZnO powder was in hexagonal wurzite phase (Jabeen, et al., 2014; Rana, et al., 2010). High crystallinity can enhance the photocatalysis performance of ZnO photocatalyst by retarding e^-/h^+ pair recombination and producing more reactive species for effective reaction with target pollutant (Hoffman, 2013; Khan, et al., 2015; Lin, et al., 2015).

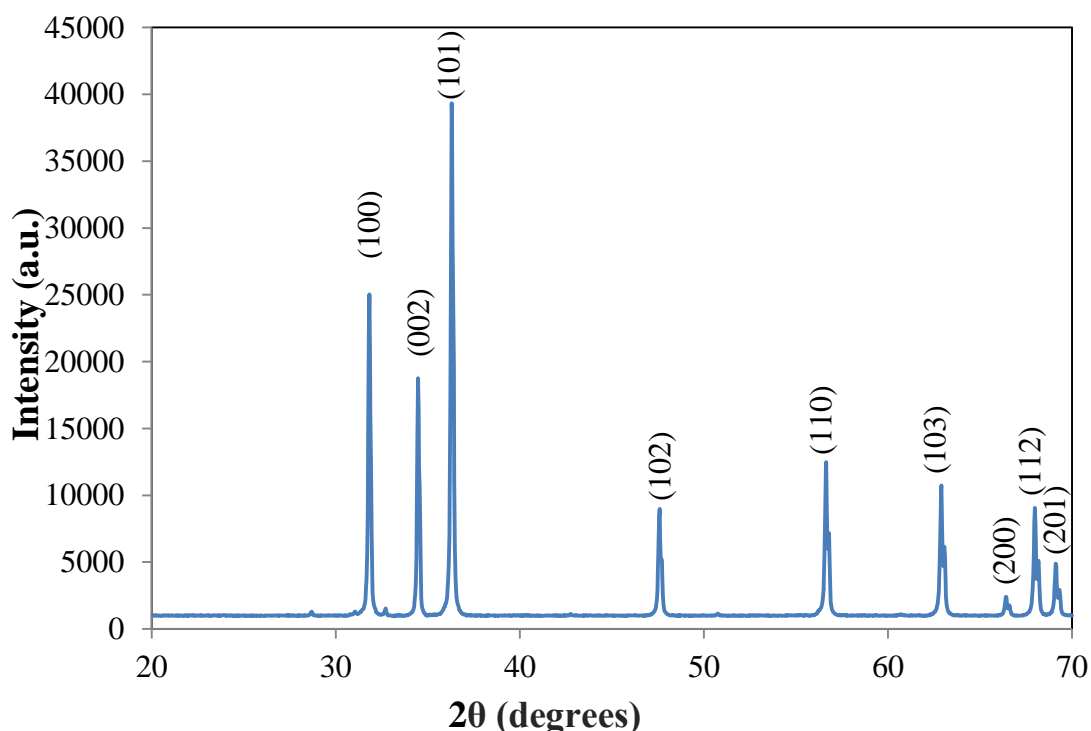


Figure 4.1: XRD Spectrum of ZnO Photocatalyst.

4.1.2 FESEM-EDX Analysis

Figures 4.2a and 4.2b show the FESEM images of commercial ZnO powder under different magnifications. As shown in the figures, commercial ZnO had irregular hexagonal shape, which was in accordance with other literature works (Yin, et al., 2016; Giri, et al., 2011). The size of one particle of ZnO was estimated to be about 160 nm to 680 nm by the FESEM, which was similar to the reported values by Hong, et al. (2016) and Giri, et al., (2011).

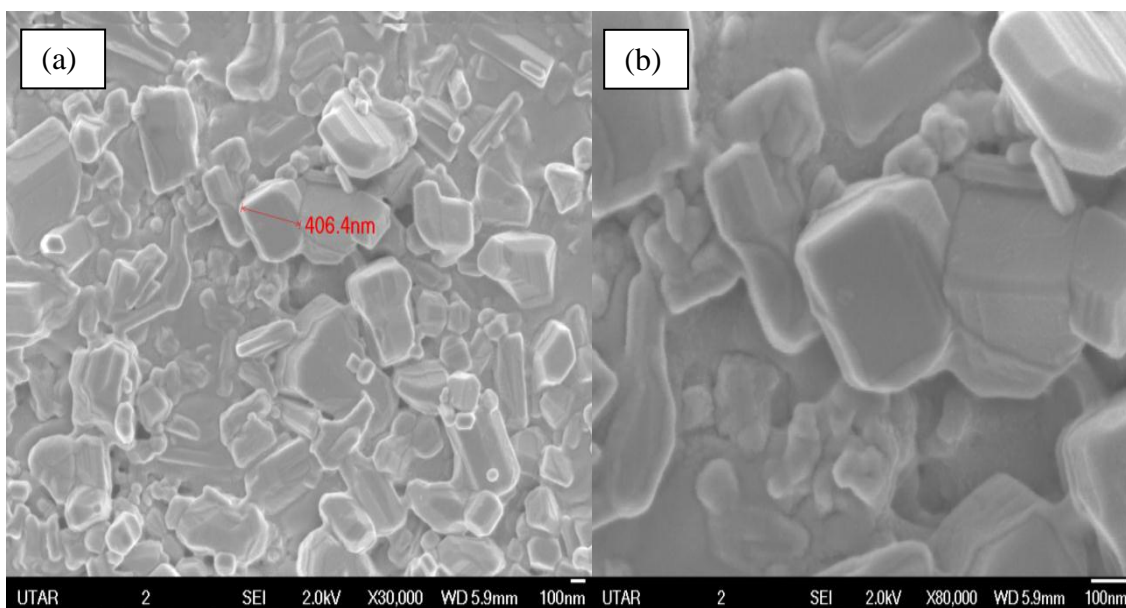


Figure 4.2 (a): FESEM Image of ZnO Powder at magnification of: (a) 30,000x, (b) 80,000x.

Figure 4.3 shows the EDX spectrum of commercial ZnO powder and its elemental composition in atomic weight %. The peaks confirmed the presence of Zn and O in the sample. Similar EDX findings have also been reported in literature works (Kumar, et al., 2013; Nejati, Rezvani & Pakizevand, 2011).

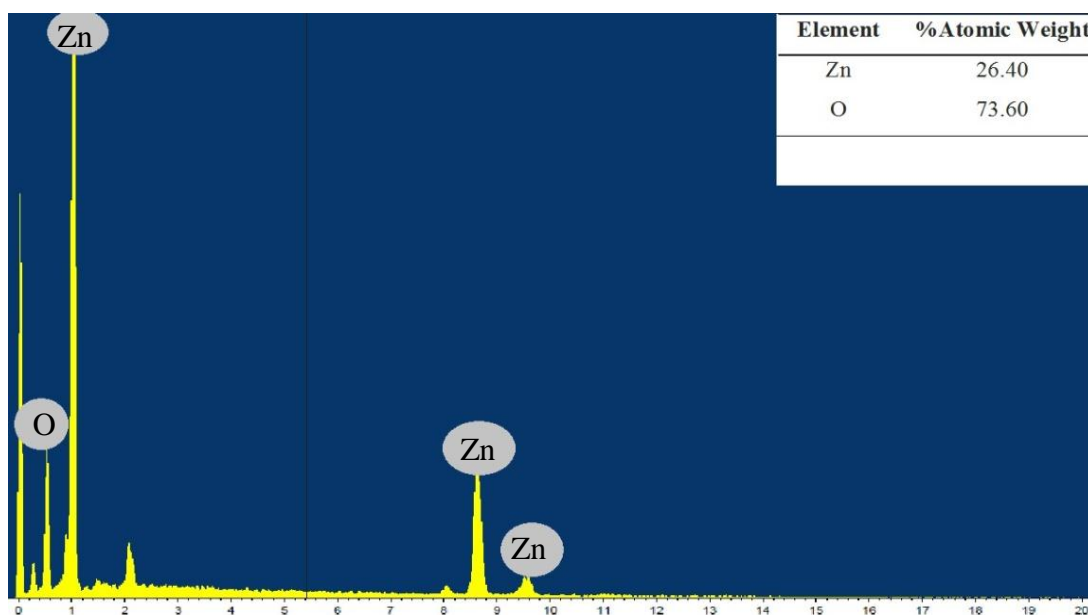


Figure 4.3 EDX Spectrum of ZnO Powder.

In this study, ZnO powders after photocatalytic reaction at different salinity concentration were collected to carry out the elemental analysis. Figures 4.4a, b and c show the EDX spectra of the collected ZnO at 50 mM salinity, 200 mM salinity and 800 mM salinity, respectively, and the elemental composition in terms of % atomic weight. It was noted that presence of Cl element was only detected in the ZnO collected after the reaction in salinity concentration equals to 800 mM. This could be due to the amount of chlorine existed in ZnO at 50 mM and 200 mM salinity concentration was in such a trace amount that it did not constitute significant amount of the total composition.

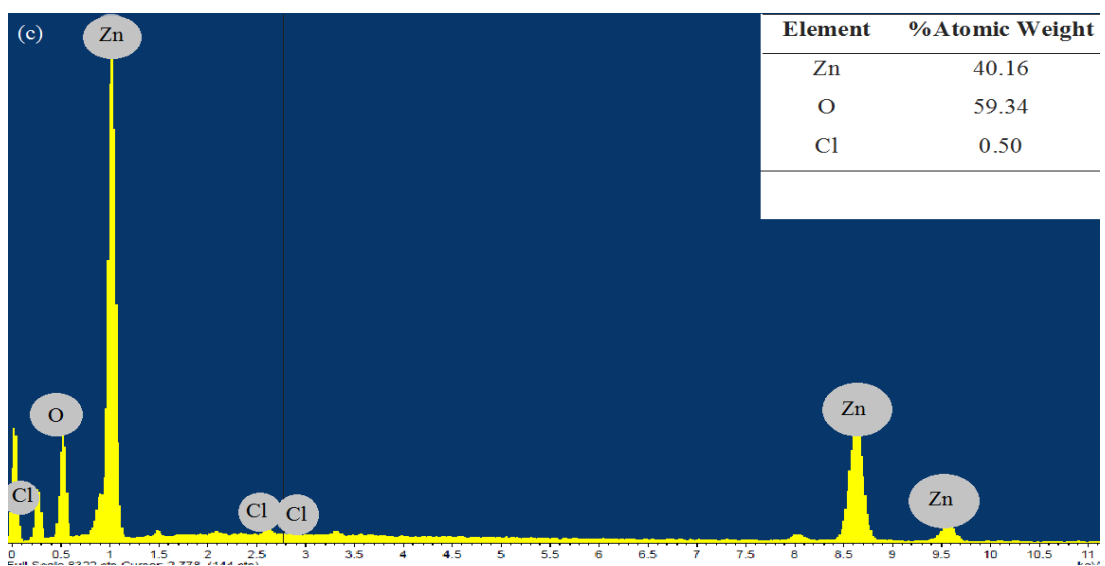
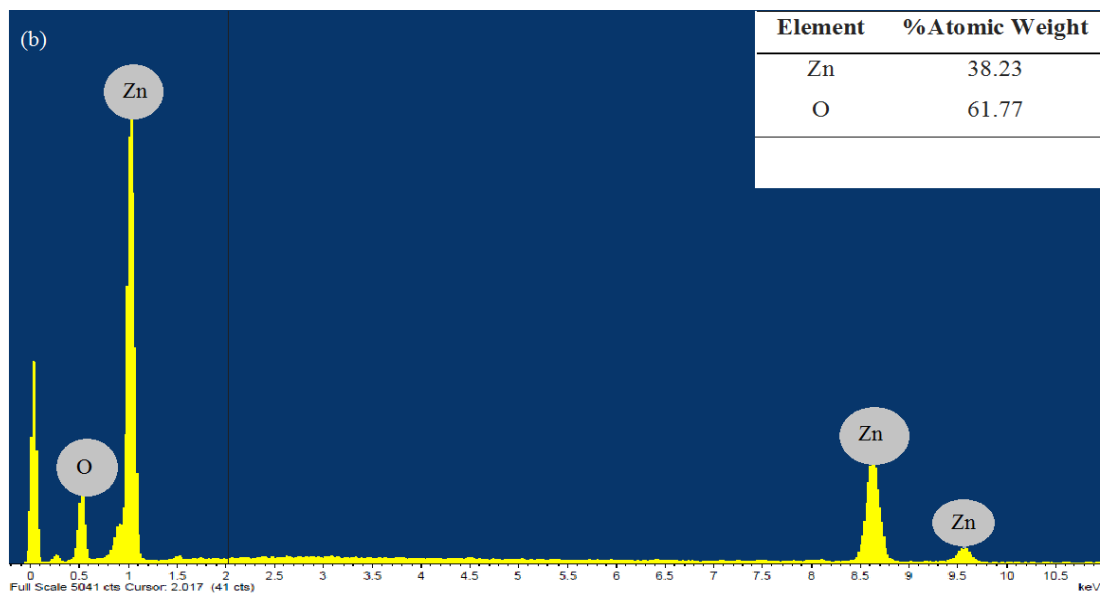
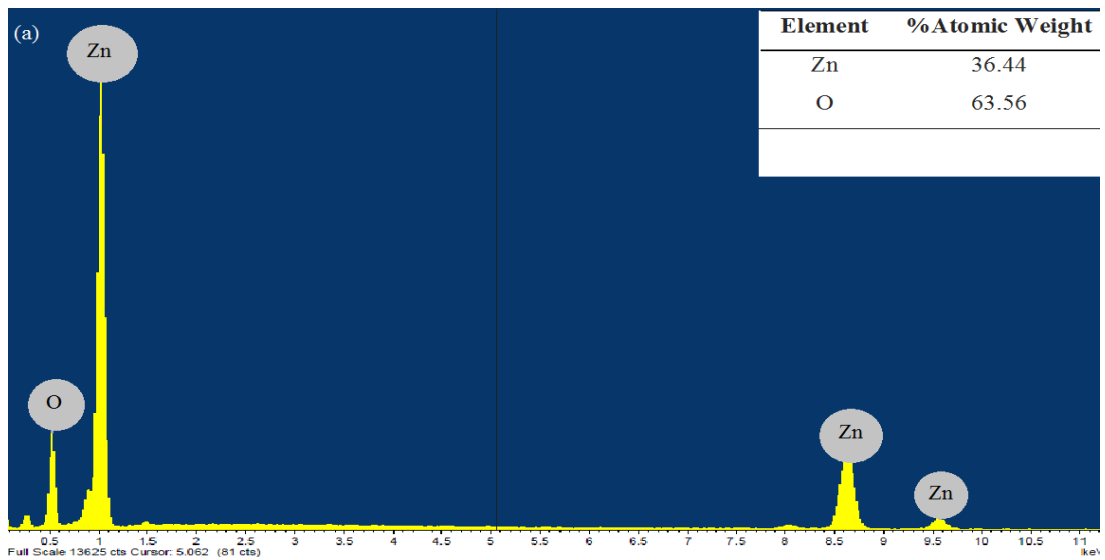


Figure 4.4: EDX Spectrum of ZnO Sample Treated at Different Salinity Concentration: (a) 50 mM, (b) 200 mM, (c) 800 mM.

4.1.3 UV-Vis Absorption Analysis

Figure 4.5 exhibits the UV-Vis absorption spectrum of ZnO photocatalyst. As shown in the figure, ZnO photocatalyst absorbed wavelength in the UV region and reached a maximum absorption at a wavelength of 364 nm. The band gap energy (E_g) of ZnO was calculated in this analysis using the absorption cut-off edge. The tangent to the cut-off edge of the spectrum was extrapolated to the x-axis to obtain the absorption edge (λ_g) of ZnO. The E_g was then calculated using the obtained λ_g with Eq. 4.1 (Jia, et al., 2016; Liu et al., 2014; Hu & Chen, 2015).

$$E_g = \frac{1240}{\lambda_g} \quad (4.1)$$

Where E_g = band gap energy of photocatalyst (eV) and λ_g = absorption edge of photocatalyst (nm).

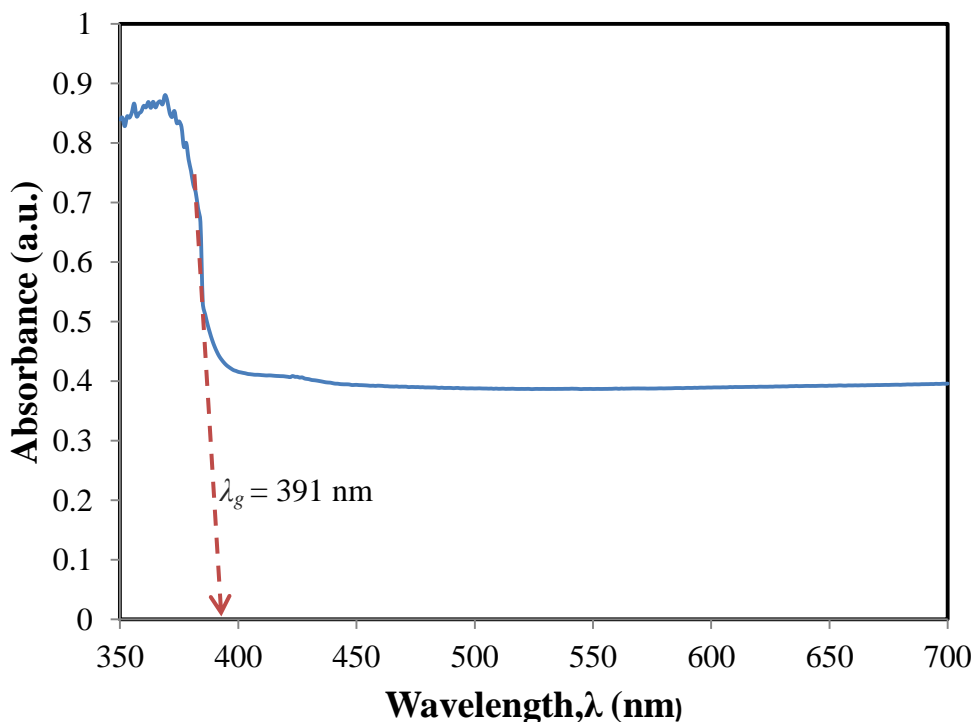


Figure 4.5: UV-Vis Absorption Spectrum of ZnO photocatalyst.

As exhibited in Figure 4.5, the estimated λ_g is 391 nm which corresponds to $E_g = 3.17$ eV that was in good agreement with reported value of $E_g = 3.2$ eV in the literatures (Lee, et al., 2016; Jia, et al., 2016).

4.2 Photocatalytic Degradation of MO-1 using ZnO under UV-Vis Light Irradiation

Photocatalytic experiments were performed to examine the catalytic activity of ZnO photocatalyst in the UV-Vis degradation of MO-1 in the presence of 200 mM chloride (Cl⁻) ions. Figure 4.6a depicts the UV-Vis absorption spectra of MO-1 which undergone UV-Vis/ZnO photocatalysis at different time intervals. The absorption peak at about 370 nm corresponding to MO-1 molecules, decreased gradually as the exposure of time increased and disappeared after 160 minutes of UV-Vis/ZnO photocatalysis. The decrease in absorbance indicated the reduction in MO-1 concentration in the solution. The reduction in MO-1 concentration was observed where the colour of the solution changed from yellow colour to nearly colourless as shown in Figure 4.6b. Similar results were obtained in studies of removal of MO-1 conducted by Chen, et al. (2009) and Seddigi (2010). Figure 4.6a also showed that the peaks of the spectra occurred consistently at wavelength equals to ~370 nm. Chen, et al. (2009) reported that the gradual reduction of the peaks at wavelength= ~370nm indicating the breakage of N=N bond of MO-1 which led to colour removal.

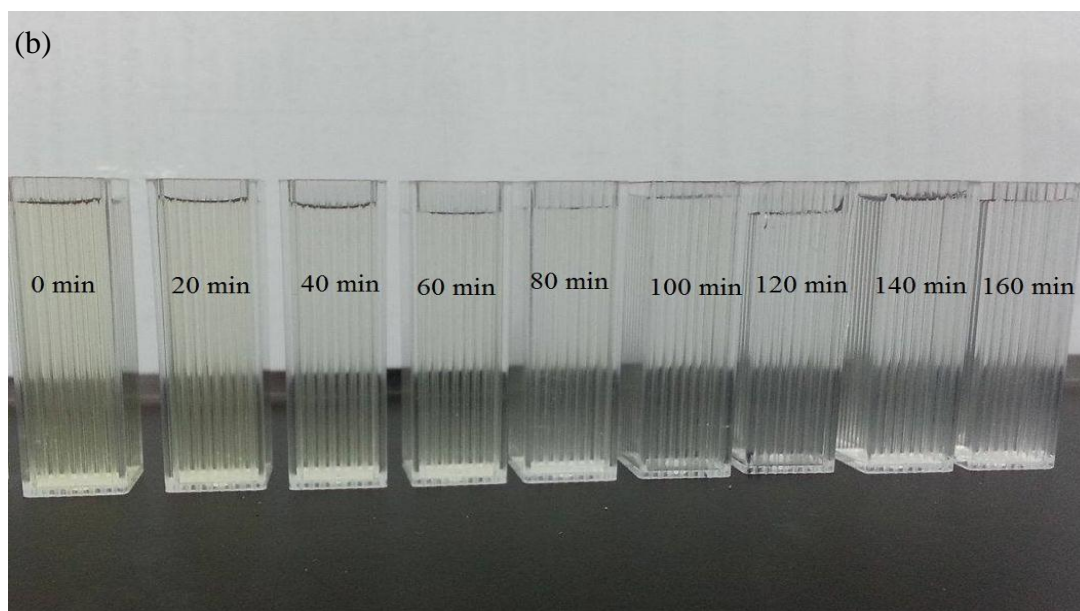
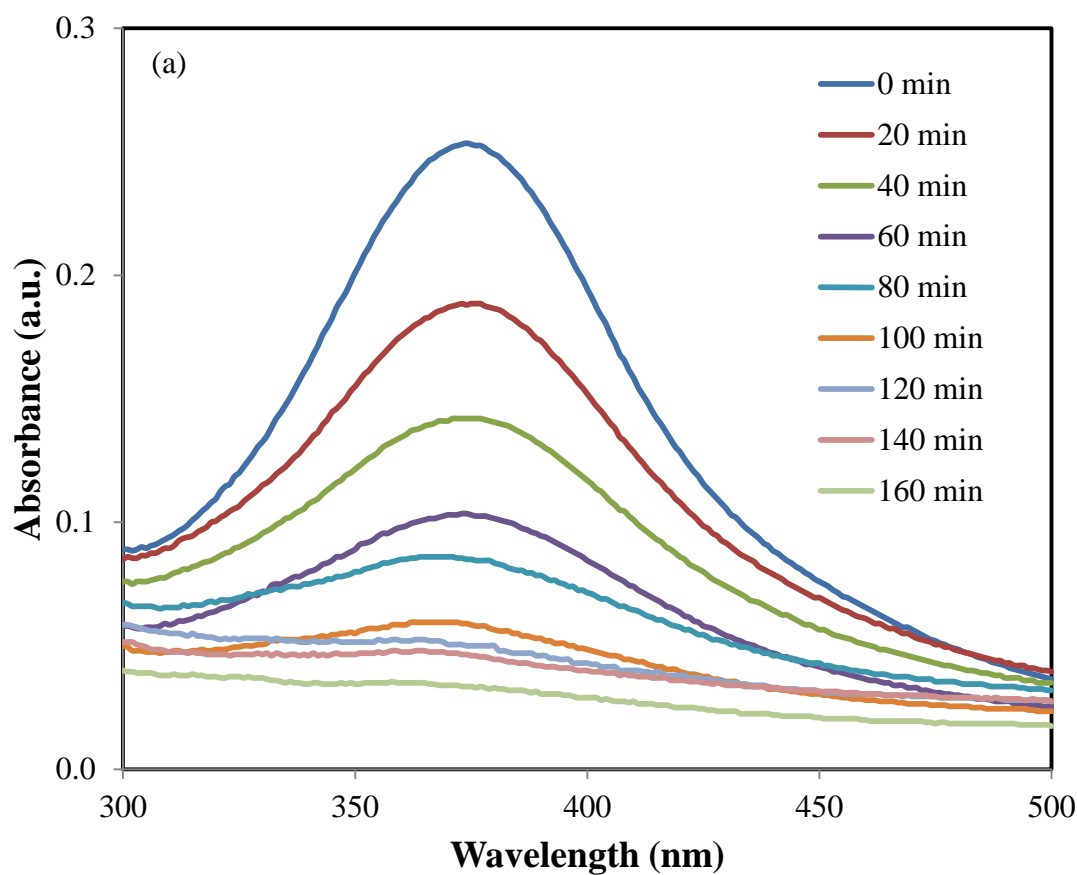


Figure 4.6 (a): UV-Vis Absorption Spectra of MO-1 Dye Contained 200 mM Cl⁻ Solution Using UV-Vis/ZnO at Different Time Intervals and (b): The Colour Change of MO-1 Dye Contained 200 mM Cl⁻ Solution Using UV-Vis/ZnO at Different Time Intervals ([MO-1] = 5 mg/L; ZnO loading = 1.0 g/L; Solution pH = 5.6).

Figure 4.7 displays the degradation % of MO-1 using photolysis, dark/ZnO, UV-Vis/ZnO and TiO₂/ZnO. As can be seen from the figure, there was no significant MO-1 degradation (2.86 %) in the photolysis process. This showed that MO-1 was stable in the presence of UV-Vis light without underwent significant degradation. In a study conducted by Aliouche, Djebbar & Sehili (2015), it was also reported that photolysis has little influence on the degradation of MO-1. Subsequently, dark adsorption was performed using ZnO photocatalyst in the absence of UV-Vis light. The adsorption of MO-1 by catalyst reached 46.87% after 120 minutes of stirring time. Subsequently, photocatalysis was carried out using UV-Vis/ZnO and UV-Vis/TiO₂ under saline condition and has achieved a degradation of 91.73 % and 81.29 %, respectively after 160 minutes of UV-Vis light irradiation. The results exhibited that UV-Vis/ZnO was more efficient than that of UV-Vis/TiO₂ in degrading MO-1 under saline condition.

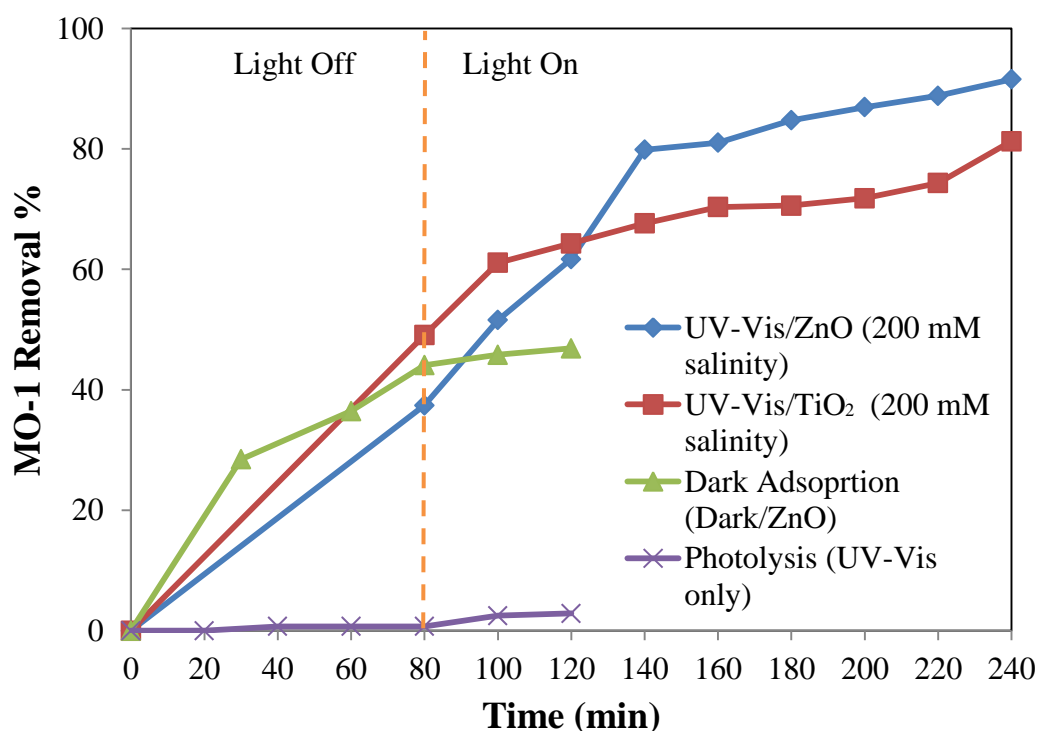


Figure 4.7: Photocatalytic experiment of MO-1 Degradation Contained 200 mM Cl using photolysis, dark/ZnO, UV-Vis/ ZnO and UV-Vis/TiO₂ ([MO-1] = 5 mg/L; Photocatalyst loading = 1.0 g/L; Solution pH = 5.6).

The photocatalytic enhancement of ZnO photocatalyst can be attributed to various factors such as crystallinity and band gap energy. Crystallinity of photocatalyst was crucial for good e^-/h^+ pair separation. As shown in the XRD spectrum present section 4.1.1, ZnO photocatalyst used in this study has high crystallinity and therefore enhanced e^-/h^+ pair separation which generated more active species to degrade MO-1. Besides, it was reported that ZnO has better absorption than TiO_2 in the UV and visible region in studies conducted by Sakthivel, et al. (2003) and Wong (2016). Thus, the higher degradation efficiency of MO-1 using ZnO photocatalyst could be attributed to its better absorption than TiO_2 .

ZnO was also well reported to have higher photocatalytic activity than TiO_2 in literature works (Krishnakumar, et al., 2010; Bizarro, 2010). In a study by Sobana & Swaminathan (2007), they found that performance of ZnO was better than TiO_2 in removing Acid Red 18 dye under similar conditions. In addition, Subash, et al. (2012) reported that ZnO removed Napthol Blue Black (NBB) dye better than TiO_2 in their study.

Additionally, sedimentation test of ZnO and TiO_2 photocatalyst after photocatalytic reaction was carried out in this study. Figures 4.8a and b exhibit the sedimentation performance of ZnO and TiO_2 in MO-1 solution, respectively after 30 minutes of settling time. It can be seen in the figure that MO-1 solution containing ZnO photocatalyst was notably less turbid than the dye solution containing TiO_2 photocatalyst. The result demonstrated that ZnO took a shorter period of time to settle in the dye solution compared to TiO_2 which enabled great possibility for ZnO photocatalyst to be recycled for reuse which made it more beneficial than TiO_2 photocatalyst. This could be added advantage of ZnO in its application in photocatalytic technology used for wastewater treatment.

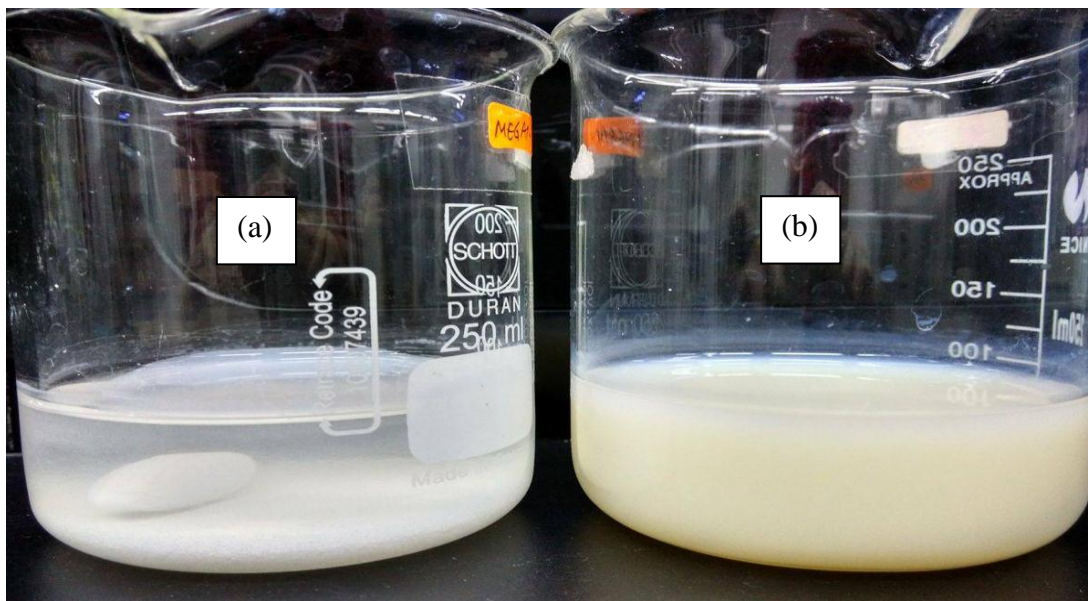


Figure 4.8: Sedimentation for 30 min in MO-1 Solution After UV-Vis Light Irradiation: (a) ZnO and (b) TiO₂ photocatalyst.

4.3 Effect of Process Parameters Studies

4.3.1 Effect of Salinity Concentration

The effect of salinity concentration on the degradation of MO-1 using ZnO photocatalyst was determined by altering the concentration of Cl⁻ ions (50-800 mM) present in the dye solution. The experiments were conducted under fixed conditions of initial MO-1 concentration of 5 mg/L, catalyst loading of 1 g/L and at natural solution pH of 5.6.

Figure 4.9 depicts the degradation percentage of MO-1 at distinct salinity concentrations using ZnO photocatalyst after UV-Vis light irradiation time of 160 minutes. As shown in the figure, degradation percentage of dye increased as salinity concentration doubled from 50 mM salinity to 100 mM and reached an optimum at 200 mM salinity with a degradation percentage of 91.73 %. As the salinity concentration continued to double above 200 mM salinity, the dye degradation

percentage decreased notably with percentage of degradation equals to 90.2% and 84.47% at 400 mM and 800 mM salinity, respectively.

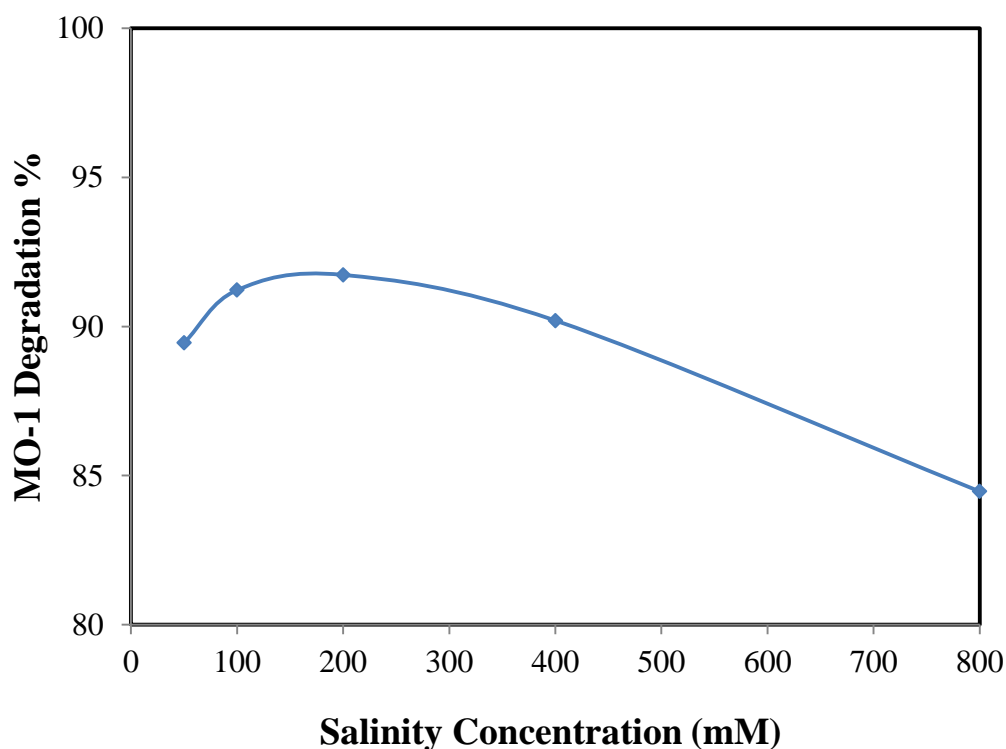


Figure 4.9: Effect of Salinity Concentration on MO-1 Degradation Using ZnO Photocatalyst ([MO-1]= 5 mg/L; ZnO Loading = 1 g/L; Solution pH = 5.6).

The effect of salinity concentration on MO-1 degradation clearly showed the double effects of Cl^- ions in enhancing photocatalytic degradation at lower concentration and its inhibitory effect at higher concentration. Yuan, et al. (2012) suggested that the boosted photocatalytic degradation of MO-1 at lower salinity concentration could be attributed to the degradation mechanism involving chlorine radicals. The formation of chlorine radicals involved in photocatalytic degradation such as chlorine radical ($\text{Cl}\cdot$) and dichloride radical ($\text{Cl}_2\cdot^-$) took place according to the reactions as shown in Eqs. (4.1) to (4.4). As shown in Eq. (4.1), Cl^- ion can react with $\cdot\text{OH}$ radical to form $\text{HOCl}\cdot^-$ radical which can subsequently form $\text{Cl}\cdot$ radical in the way shown in Eq. (4.2). Moreover, $\text{Cl}\cdot$ radical can be formed directly by reaction between Cl^- ion and $\cdot\text{OH}$ radical as exhibited in Eq. (4.3). In addition, $\text{Cl}\cdot$ radical can react with Cl^- ion to form $\text{Cl}_2\cdot^-$ radical. Thus, the presence of the additional $\text{Cl}\cdot$ and

$\text{Cl}_2\cdot^-$ radicals alongside with other radicals such as hydroxyl radicals ($\cdot\text{OH}$), superoxide radicals ($\text{O}_2\cdot^-$) and hydroperoxyl radicals, ($\text{HO}_2\cdot$), managed to enhance the photocatalytic degradation of MO-1. Figure 4.10 shows the degradation mechanism of dye photocatalysis on ZnO photocatalyst in the existence of Cl^- ions (Yuan, et al., 2012; Lee, et al., 2016; Wang, Lu & Feng, 2013).

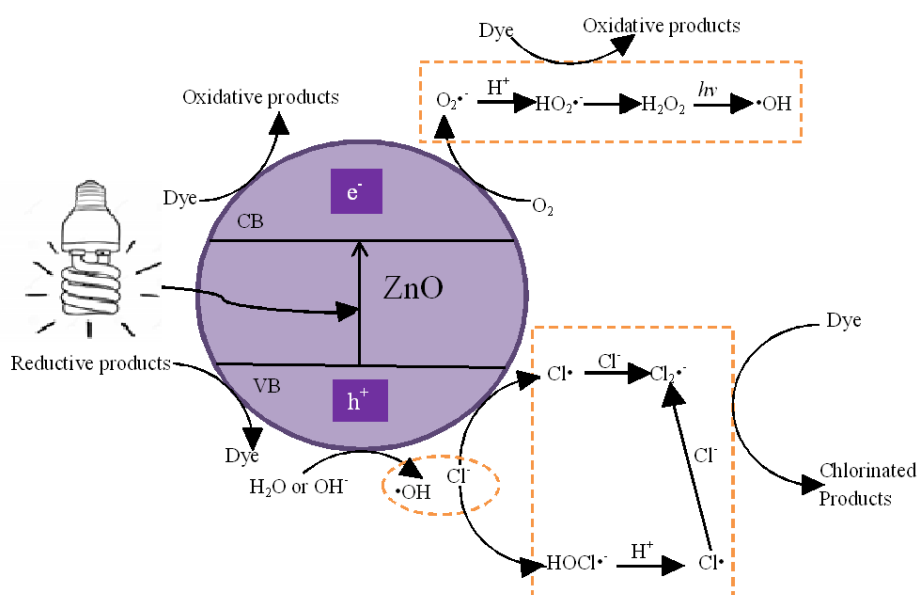


Figure 4.10: Proposed Degradation Mechanism of ZnO Photocatalyst in The Presence of Cl^- ions.

In addition, the enhancement in degradation performance at lower salinity concentrations could be due to the improved adsorption of dye molecules onto ZnO surface at natural pH solution. In this part of the study, the experiment was carried out at natural solution pH of pH 5.6 which is in acidic condition. At pH 5.6, the

surface of ZnO photocatalyst was positively-charged due to the lower pH compared to the point of zero charge (PZC) of ZnO. PZC refers to the pH where the surface charge of photocatalyst will be zero. The PZC of ZnO photocatalyst has been reported to be pH~ 9.0 (Habibi & Rahmati, 2015; Jia, et al., 2016). Therefore, at pH 5.6 (< PZC), ZnO surface was positively-charged. This caused adsorption of anionic MO-1 molecules onto positively-charged ZnO surface due to electrostatic attraction at low Cl⁻ concentrations. Improved adsorption on photocatalyst surface enabled more effective degradation of MO-1 molecules by forming oxidative and reductive products that can be further degraded. The improved adsorption of MO-1 molecules on ZnO photocatalyst was supported by the high adsorption achieved as exhibited in Figure 4.8. The enhancement effect of Cl⁻ on photocatalytic degradation was scarcely reported in the literatures (Assi, et al., 2014; Wang, Lu & Feng, 2013; Yuan et al., 2012). This might be due to the limited range of salinity concentrations selected by other researchers.

However, at higher salinity concentrations, inhibitory effect on photocatalytic degradation was observed in this study. This could be due to larger amount of anionic Cl⁻ ions were adsorbed on ZnO surface which caused competition with dye molecules and other compounds such as H₂O and O₂ in binding to limited active sites on the photocatalyst. Therefore, the more prominent inhibitory effect of Cl⁻ at high concentration of 800 mM could be explained. This finding was also supported by the EDX result at section 4.1.2 where the chlorine element was detected in the ZnO photocatalyst after the photocatalytic reaction. In a study conducted by Santiago, et al. (2014), they reported that the adsorption of other molecules such as water molecules on the photocatalyst decreased which supported the hindrance of photocatalytic degradation efficiency by Cl⁻ ions in their Fourier Transform Infrared Spectroscopy (FT-IR) findings. Similar inhibitory effects of Cl⁻ at higher concentrations were presented in study carried out by Assi, et al., (2014) and Wang, Lu & Feng (2013). Assi, et al. (2014) has reported the retardation effect of Cl⁻ in the degradation of *ortho*-nitrophenol at Cl⁻ concentration of ~400 mM using ZnO photocatalyst. Besides, Wang, Lu & Feng (2013) have also reported the inhibitory in degradation of another anionic dye, Methyl Orange at higher salinity concentration in their study using polyoxometalate yttrium-doped TiO₂ photocatalyst.

In overall, the MO-1 dye degradation may be attributed to a chlorine radicals-mediated mechanism. 200 mM of Cl^- ions gave the ideal degradation efficiency and therefore this Cl^- ion concentration was selected for subsequent experiment.

4.3.2 Effect of Initial Dye Concentration

The influence of initial MO-1 concentration was determined in this study by varying the initial dye concentration from 2.5 mg/L to 20 mg/L. The experiments were conducted under fixed conditions of photocatalyst loading of 1 g/L and at natural solution pH of 5.6.

Figure 4.11 presents the effect of initial MO-1 concentration on degradation percentage of MO-1 using ZnO photocatalyst. It was observed from the figure that as the initial dye concentration increased, the degradation percentage decreased markedly. The best initial MO-1 concentration determined was 2.5 mg/L which achieved the highest degradation percentage of 92.37 % after 160 minutes of UV-Vis light irradiation. For higher initial MO-1 concentration at 5 mg/L, 10 mg/L and 20 mg/L, the achieved degradation percentage were 89.33 %, 76.36 % and 46.45 %, respectively at similar light irradiation time.

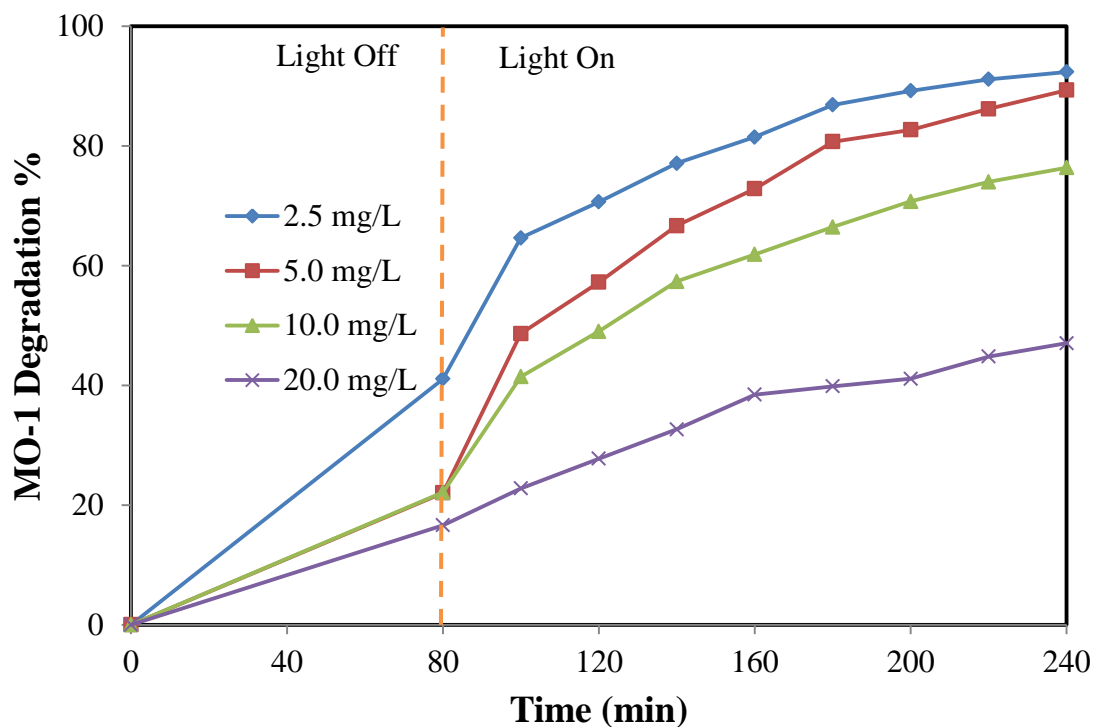


Figure 4.11: Effect of Initial Dye Concentration on MO-1 Degradation Percentage (ZnO Loading = 1.0 g/L; Salinity Concentration = 200 mM; Solution pH = 5.6).

The experimental observations showed that the increased in initial dye concentration deteriorated the photocatalytic degradation of MO-1. It was widely reported the declined percentage of photocatalytic degradation was caused by lesser amount of photons reaching the photocatalyst surface (Lee, et al., 2016; Abass & Raof, 2016; Kulkarni & Thakur, 2014). When the initial dye concentration increased, colour intensity of solution increased. This subsequently led to lesser penetration of UV-Vis light into the solution and reduced light that could reach the surface of ZnO photocatalyst to generate e^-/h^+ pair and other reactive species. Furthermore, it was also reported that the higher number of dye molecules present in the solution at high initial dye concentration could have competition with molecules such as H_2O and O_2 for limited active sites on ZnO photocatalyst surface. This could reduce the number of radicals generated attributable to lesser active sites available for adsorption of H_2O and O_2 (Hayat, et al., 2010; Habib, et al., 2013).

The findings from present study were also consistent with the photocatalytic test that used the same MO-1 dye (Abass & Raouf, 2016; Seddigi, 2010). Abass & Raouf (2016) has reported a decrease in dye removal percentage from ~90% to ~60% when initial MO-1 dye concentration was increased from 40 mg/L to 60 mg/L using synthesized ZnO photocatalyst. In addition, the study conducted by Seddigi (2010) revealed that the increase of initial MO-1 dye concentration from 50 mg/L to 400 mg/L reduced the photocatalytic degradation percentage from 80% to almost 0%. Consequently, a low initial concentration of 2.5 mg/L can be taken as the best degradation of MO-1.

4.3.3 Effect of Solution pH

The effect of solution pH on the degradation of MO-1 using ZnO photocatalyst was studied by varying the solution pH from pH 3.1 to pH 10.4. The experiments were conducted under fixed conditions of initial MO-1 concentration of 2.5 mg/L and photocatalyst loading of 1 g/L.

Figure 4.12 presents the effect of solution pH on the photocatalytic degradation of MO-1. As exhibited in the figure, the optimum pH which corresponded to the highest degradation percentage of 92.37 % was pH 5.6, which is the natural pH. Additionally, the percentages of degradation at pH 3.2 and pH 7.2 were comparable and gave a value of 85.74 % and 83.72 %, respectively. The MO-1 degradation was least efficient at pH 10.2 with a degradation percentage of 78.11 %.

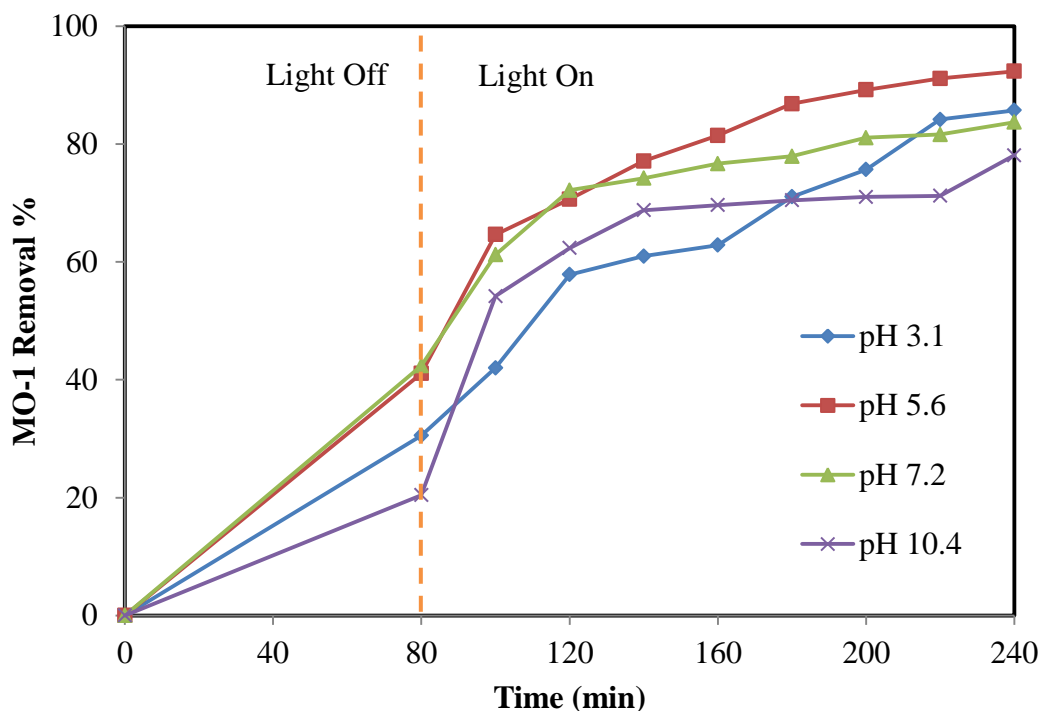


Figure 4.12: Effect of Solution pH on MO-1 Degradation Percentage ([MO-1]= 2.5 mg/L; ZnO Loading = 1.0 g/L; Salinity Concentration= 200 mM).

The concept of point of zero charge (PZC) was used widely to describe the influence of solution pH on the photocatalytic degradation reaction. The results clearly showed that the degradation of MO-1 was most effective at natural solution pH of pH 5.6 with no prior adjustment. At pH below the PZC of ZnO (pH 9), the surface of the photocatalyst was positively-charged. At pH 5.6, the positively-charged surface of ZnO encouraged the adsorption of anionic MO-1 molecules onto the surface of photocatalyst where degradation took place. Tiwari, et al. (2015) reported that at low pH condition, the scavenging of $\bullet\text{OH}$ by H^+ was dominant due to the presence of high amount of H^+ in acidic condition. At pH 5.6, the scavenging of $\bullet\text{OH}$ is less dominant as no pH adjustment was performed which indicated that there was no addition of H^+ into the dye solution. This evidently explained the higher degradation percentage at pH 5.6 compared to that at pH 3.1. Scavenging of $\bullet\text{OH}$ by H^+ was likely to be dominant at pH 3.1 which cause a declined in photocatalytic degradation percentage of MO-1.

The results also exhibited that all pH below the PZC of ZnO have higher percentage of degradation compared to pH 10, which was higher than the PZC. This could be explained by the surface charge of ZnO at pH higher than PZC of ZnO. At pH 10 (>PZC), the surface of ZnO was negatively-charged and this created electrostatic repulsion between dye molecules, other anions such as OH⁻ and Cl⁻ and the negatively-charged surface of ZnO photocatalyst. This possibly reduced the degradation of dye molecules at the photocatalyst surface and production of •OH through reaction of OH⁻ and h⁺ (Tiwari et al., 2015; Hayat, et al., 2010).

Similar results have been reported in studies carried out by Hayat, et al. (2010) and Tiwari, et al. (2015) where highest MO-1 degradation percentage was obtained at the natural pH solution with value of 80.00 % and 90.00%, respectively. Therefore, the natural pH of 5.6 was chosen as the optimum natural pH solution for degradation of MO-1.

4.4 Mineralization of MO-1

The complete mineralization is an important criterion in the treatment of organic pollutants present in wastewater. The mineralization efficiency of MO-1 using UV-Vis/ZnO photocatalysis in optimized condition was determined using Chemical Oxygen Demand (COD) test. Figure 4.13 shows the MO-1 degradation and COD removal at different time interval. As can be seen in the figure, COD removal increased progressively during the 240 minutes of UV-Vis irradiation. This confirmed the mineralization of MO-1 resulting from breakdown of MO-1 molecules and its intermediates. COD removal reached 67.09% at the point where degradation achieved 92.37% (160 minutes UV-Vis irradiation) which indicated that intermediates were still present in the MO-1 solution. It was also observed that, COD removal only reached up to 72.01% when the irradiation time was elongated to 240 minutes. These findings evidently showed that mineralization required a longer time than degradation (Joshi & Shrivastava, 2012; Li, et al., 2011).

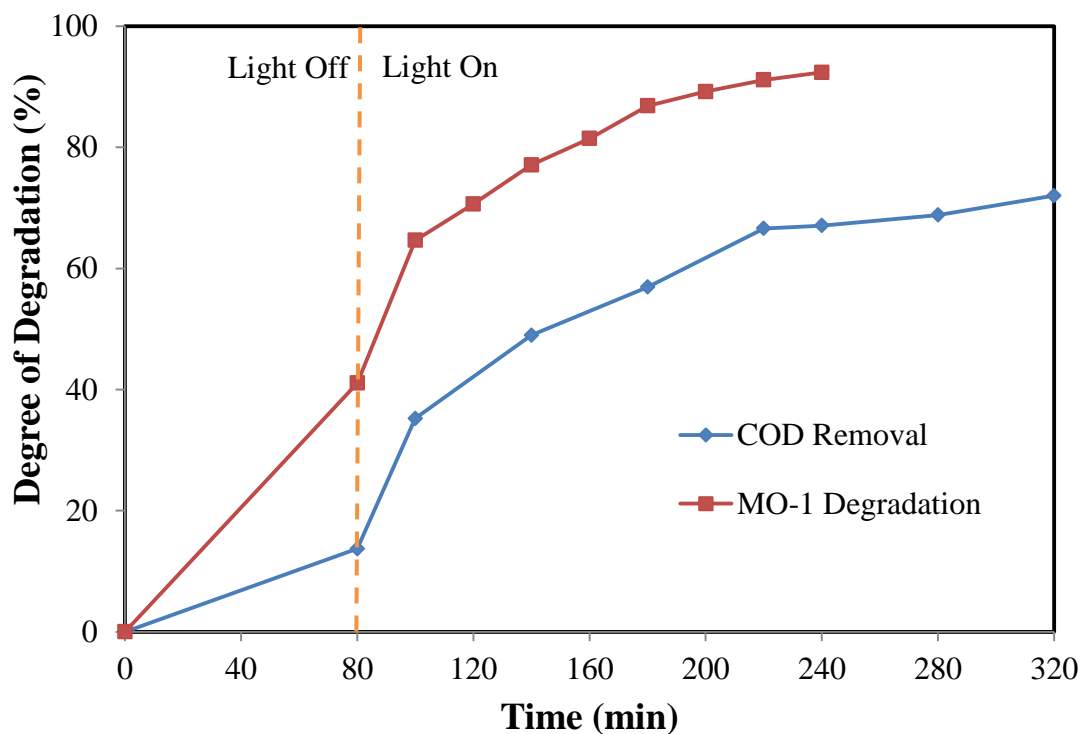


Figure 4.13: Variation of MO-1 and COD Percentage using UV-Vis/ZnO in presence of 200 mM Cl⁻ ions ([MO-1] = 2.5 mg/L; ZnO Loading = 1.0 g/L; Solution pH = 5.6).

Similar results have been obtained in studies involving other dyes conducted by Soltani, et al. (2015) and Kamani, et al. (2015). Soltani, et al (2015) reported a COD removal of 81% at 100% colour removal of MB. Furthermore, it was revealed in Kamani, et al. (2015) study that the COD removal percentage achieved was ~90% when colour removal percentage of 96% has been reached in the degradation of Sulphur Red 14 after 50 minutes of treatment.

4.5 Kinetic Study

4.5.1 Photocatalytic Degradation Kinetics of MO-1

Kinetic study was conducted in this research to determine the reaction kinetic characteristics such as reaction rate of photocatalytic degradation of MO-1 in saline condition using ZnO photocatalyst. In heterogeneous photocatalytic reaction, rate law was employed to determine the reaction rate which can be expressed as shown in Eq. (4.5).

$$r = -\frac{dC}{dt} = kC^n \quad (4.5)$$

which k represents the rate constant, C represents the reactant concentration and n represents the order of reaction.

The photocatalytic degradation rate is able to be influenced by several factors such as initial substrate concentration, solution pH, catalyst loading and light intensity (Hayat et al., 2010; Jia, et al., 2016). In the present study, the effect of initial MO-1 concentration (2.5-20.0 mg/L) on the rate of reaction was studied. The experiment was carried out at fixed conditions of ZnO loading = 1.0 g/L, salinity concentration = 200 mM and solution pH = 5.6.

In literatures, the photocatalytic degradation reaction of organic pollutants obeys the first-order kinetics (Pung, Lee & Aziz, 2012; Abass, et al., 2016). Therefore, first-order kinetics was employed in this study to determine the apparent rate constant, k_{app} at different initial MO-1 concentrations. Knowing the reaction order ($n = 1$), Eq. (4.5) can thus be expressed in the form as shown in Eq. (4.6).

$$-\frac{dC}{dt} = k_{app} C \quad (4.6)$$

Subsequently, Eq. (4.6) which was integrated from Eq. (4.5) can be used to determine the k_{app} of the reaction at different initial dye concentration.

Figure 4.14 shows the plot of $\ln C_0/C$ vs. t of MO-1 at different initial dye concentrations. The values k_{app} and correlation coefficient, R^2 at different initial MO-1 concentrations were summarized in Table 4.1. As can be seen from Figure 4.17 and Table 4.1, k_{app} decreased with increased initial dye concentration. This was due to the similar reason discussed in section 4.3.2 where increase in initial dye concentration led to higher competition between dye molecules in adsorbing onto ZnO photocatalyst surface. As shown in Figure 4.17 and Table 4.1, the kinetic data was in accordance well with all R^2 values larger than 0.9.

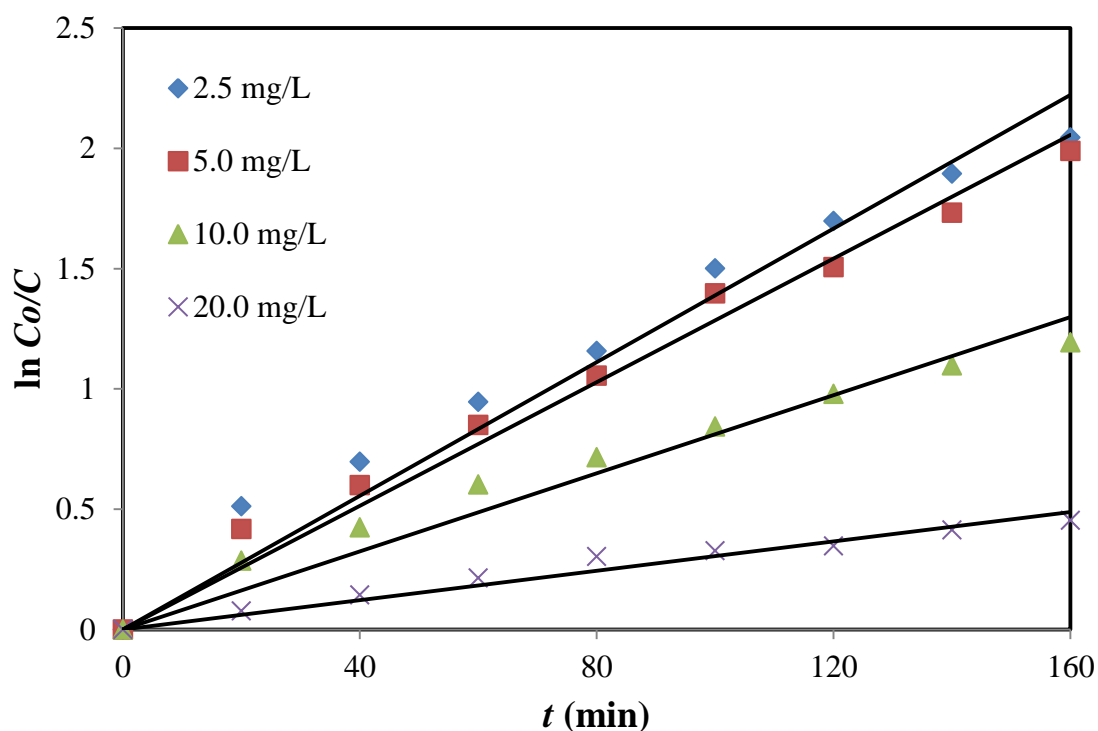


Figure 4.14: Kinetics of Photocatalytic Degradation of MO-1 at Different Initial Dye Concentrations. (ZnO loading = 1.0 g/L; Salinity concentration = 200 mM; Solution pH = 5.6).

Table 4.1: The k_{app} and R^2 values at Distinct Initial MO-1 Concentrations.

Initial MO-1 Concentration (mg/L)	k_{app} (min^{-1})	R^2
2.5	0.0139	0.9636
5.0	0.0129	0.9816
10.0	0.0081	0.9547
20.0	0.0031	0.9617

Other literature works have reported similar findings in photocatalytic degradation of dyes where the k_{app} decreased with the increase of initial dye concentration (Tiwari, et al., 2015; Abass & Raoof, 2016; Krishnakumar, et al., 2010). A comparison study was made between the present study and other work regarding on k_{app} values. The results were shown in Table 4.2. It was noted that the k_{app} of present study was comparable with the reported values in a study conducted by literature studies.

Table 4.2: The k_{app} values obtained in the photocatalytic degradation of dyes.

Dye	Photocatalyst	Initial Concentration (mg/L)	k_{app}	References
Mordant Orange-1	ZnO	2.5	0.0139	Present Study
		5.0	0.0129	
		10.0	0.0081	
		20.0	0.0031	
Mordant Orange-1	ZnO	40.0	0.0190	Abass & Raoof, 2016
		50.0	0.0110	
		60.0	0.0080	
Mordant Orange-1	TiO ₂	1.0	0.009	Tiwari, et al., 2015
		5.0	0.0042	
		10.0	0.00240	
		15.0	.0019	
		20.0	0.0015	
Acid Black 1	ZnO	0.6	0.0690	Krishnakumar, et al., 2010
		1.2	0.0500	
		1.9	0.0320	
		2.5	0.0200	
		3.1	0.0100	

4.5.2 Langmuir-Hinshelwood (L-H) Kinetic Model

It was widely reported that photocatalytic degradation rate of organic pollutants complied the Langmuir-Hinshelwood (L-H) kinetic expression (Habib, et al., 2013; Jia, et al., 2016; Assi, et al., 2014). Therefore, L-H kinetic model was used in this

study to determine the initial photodegradation rate of MO-1 in saline condition. The L-H expression can be expressed as shown in Eq. (4.7).

$$r = - \frac{dC}{dt} = \frac{k_{L-H}KC}{1+KC} \quad (4.7)$$

which r is the initial rate of photocatalytic degradation (mg/L•min), C is equal to C_o when $t=0$ where C_o is the concentration of MO-1 after dark adsorption of 80 minutes (mg/L), k_{L-H} is the rate constant of photocatalytic reaction (mg/L•min) and K is the adsorption equilibrium constant (L/mg), respectively.

In the photocatalytic system, the L-H expression can be simplified into the first-order form as shown in Eq. (3.4) previously presented in section 3.7. It can be further expressed in terms of r as shown in Eq. (3.5) present in section 3.7, where the MO-1 concentration was assumed to be very low ($KC \ll 1$) (Asenjo, et al., 2013).

In this study, the initial photocatalytic degradation rate was calculated at $t = 20$ minutes. Using Eq. (3.4) in section 3.7, value of k_{L-H} and K were found through the plot of $1/r$ (L•min/mg) vs. $1/C$ (L/mg) as shown in Figure 4.15. The value of k_{L-H} and K obtained from this study were 0.1726 mg/L•min and 0.0336 L/mg, respectively. As can be seen from the figure, a linear plot with a R^2 larger than 0.9 was obtained. This confirmed that the data of this study was fitted well to the L-H kinetic model.

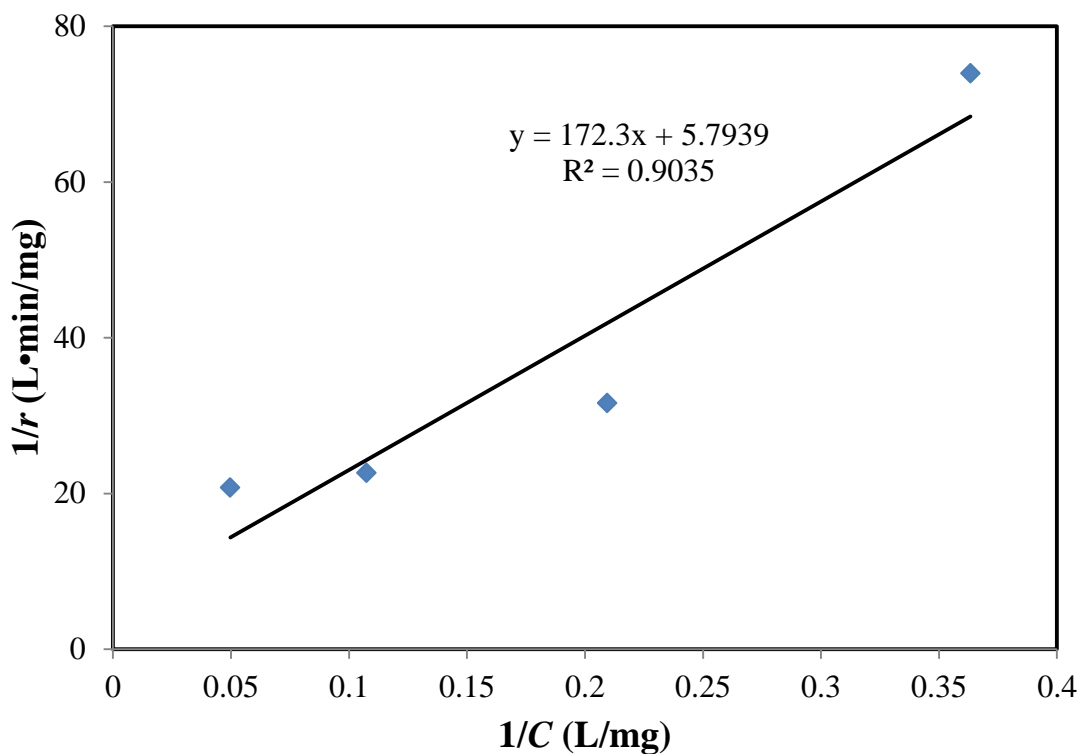


Figure 4.15: Plot of $1/r$ vs. $1/C$ of Photocatalytic Degradation of MO-1 (ZnO loading = 1g/L, Salinity concentration = 200 mM, Solution pH =5.6, t = 20 min).

Comparable results were reported in other literature works of photocatalytic degradation of organic pollutants (Khezrianjoo & Revanasiddappa, 2012; Rao, Sivasankar & Sadasivam, 2009). The values of k_{L-H} and K obtained in the present study and reported in other literature works were summarized in Table 4.3.

Table 4.3 Values of k_{L-H} and K Determined in MO-1 Degradation.

Pollutant	Photocatalyst	k_{L-H} (mg/L•min)	K (L/mg)	References
MO-1	ZnO	0.1726	0.0336	Present Study
Metanil Yellow	ZnO	1.0530	0.1550	Khezrianjoo & Revanasiddappa, (2012)
Emerald Green	TiO ₂	1.5700	0.0373	Montazerozohori, Nasr-esfahani & Jooharin (2012)
Salicyclic Acid	ZnO	2.7×10^{-6}	3.186×10^{-11}	Rao, Sivasankar & Sadasivam, (2009)

CHAPTER 5

CONCLUSION AND RECOMMENDATIONS

5.1 Conclusion

In present research, photocatalytic degradation of MO-1 dye solution in saline condition using ZnO photocatalyst under UV-Vis light irradiation has been studied. Sodium Chloride (NaCl) salt was employed in this research as it was the most common dye additive found in textile effluents. The effect of Cl^- ions on the photocatalytic degradation performance was also investigated.

Characterization studies such as XRD, FESEM-EDX and UV-Vis absorption have been conducted on ZnO photocatalyst. Through XRD analysis, ZnO was found to be in hexagonal wurzite phase with high crystallinity. Besides, it was found that ZnO has irregular hexagonal shapes from FESEM analysis and its elemental composition was confirmed by EDX analysis. The band gap energy of ZnO photocatalyst was determined using an UV-Vis absorption analysis and has found to be 3.17 eV.

Subsequently, a comparison study between performance of ZnO and commercial TiO_2 was conducted. It was found that ZnO has higher photocatalytic activity (91.73%) than TiO_2 (81.29%) under 160 minutes of irradiation. In addition, the sedimentation test revealed that ZnO particles able to perform better sedimentation ability than TiO_2 in the solution after treatment which increased the possibility of catalyst reusability in the practical application.

The effect of process parameters including salinity concentration, initial dye concentration and solution pH on the photocatalytic degradation of MO-1 were also

investigated. The findings exhibited that salinity concentration has both enhancement and inhibitory effects on the degradation efficiency MO-1. At low Cl^- ions concentration, the percentage of degradation of MO-1 increased and reached an optimum 200 mM possibly due to the chlorine radicals-mediated mechanism. Upon the optimum salinity concentration, the degradation efficiency decreased with further increase of Cl^- ions concentration. This might be due to the competition between Cl^- ions, dye molecules and other compound such as water molecules in binding to active sites on ZnO photocatalyst. This was supported by the EDX finding of the collected ZnO photocatalyst after the photocatalytic reaction at 800 mM which detected the presence of Cl element. For the effect of initial dye concentration, MO-1 degradation efficiency decreased with the increase of initial MO-1 dye concentration due to higher competition between molecules for limited active sites on ZnO photocatalyst. The solution pH effect found that the percentage of degradation at pH 3, 5.6 and 7 was higher compared to that at pH 10. The optimum experimental conditions found in this study were 200 mM salinity concentration, 2.5 mg/L initial MO-1 concentration and natural solution pH of 5.6.

In addition, mineralization study in terms of COD removal was investigated. COD removal percentage achieved 67.09 % after 240 minutes of UV-Vis light irradiation. It was found that mineralization of MO-1 took a longer time than degradation. Furthermore, kinetic study was carried out to study the kinetics of the photocatalytic degradation reaction of MO-1 in saline condition using L-H pseudo-first-order kinetic model. It was revealed that the apparent first order rate constant k_{app} decreased with an increasing initial dye concentration. The k_{L-H} and K obtained in this research were equal to 0.1726 mg/L•min and 0.0336 L/mg. Kinetic data of this study was in accordance to L-H pseudo-first-order kinetic model.

In summary, ZnO photocatalyst was effective in the degradation and mineralization of MO-1 in saline condition under UV-Vis light irradiation. This can be attributed to the high crystallinity and suitable band gap of ZnO photocatalyst. This has proven that ZnO photocatalyst has high suitability to be applied in photocatalytic degradation of organic pollutants such as azo dyes.

5.2 Recommendations

Upon completion of the present study, a few fundamentals and engineering aspects were found and require attention in the future study.

1. Performance of ZnO should be examined in degrading simulated or actual dye effluent which consists of mixture of dyes since textile effluent is mixtures of various types of organic pollutants.
2. Performance of ZnO in the presence of other salt anions other than Cl^- ions can be investigated as other salts are also commonly used in dye industry as dye additives.
3. Performance of ZnO in degrading organic pollutants using sunlight irradiation should be studied as sunlight is abundant and pollution-free.

REFERENCES

- Abass, A. and Raouf, S., 2016. Photocatalytic removal of alizarin yellow R from water using modified zinc oxide catalyst. *Asian Journal of Chemistry*, 28, pp.312-316.
- Abbas A., Murtaza S., Shadid K., Munir M., Ayub R., and Akber S., 2012. Comparative study of adsorptive removal of congo red and brilliant green dyes from water using peanut shell. *Middle –East Journal of Scientific research*, 11, pp.828 -832.
- Akpan, U. and Hameed, B., 2009. Parameters affecting the photocatalytic degradation of dyes using TiO₂-based photocatalysts: A review. *Journal of Hazardous Materials*, 170, pp.520-529.
- Aleboye, A., Kasiri, M. and Aleboye, H., 2012. Influence of dyeing auxiliaries on AB74 dye degradation by UV/H₂O₂ process. *Journal of Environmental Management*, 113, pp.426-431.
- Aliouche, S., Djebbar, K. and Sehili, T., 2015. Removal of an azo dye (Alizarin yellow) in homogeneous medium using direct photolysis, acetone/UV, H₂O₂/UV, /UV, H₂O₂//UV, and /heat. *Desalination and Water Treatment*, 57, pp.18182-18193.
- Alventosa-deLara, E., Barredo-Damas, S., Zuriaga-Agustí, E., Alcaina-Miranda, M. and Iborra-Clar, M., 2014. Ultrafiltration ceramic membrane performance during the treatment of model solutions containing dye and salt. *Separation and Purification Technology*, 129, pp.96-105.
- Arora, S., 2014. Textile dyes: It's impact on environment and its treatment. *Journal of Bioremediation and Biodegradation*, 5, pp.1.
- Asenjo, N., Santamaría, R., Blanco, C., Granda, M., Álvarez, P. and Menéndez, R., 2013. Correct use of the Langmuir–Hinshelwood equation for proving the absence of a synergy effect in the photocatalytic degradation of phenol on a suspended mixture of titania and activated carbon. *Carbon*, 55, pp.62-69.
- Balapure, K., Bhatt, N. and Madamwar, D., 2014. Mineralization of reactive azo dyes present in simulated textile waste water using down flow microaerophilic fixed film bioreactor. *Bioresource Technology*, 175, pp.1-7.

- Bindu, P. and Thomas, S., 2014. Estimation of lattice strain in ZnO nanoparticles: X-ray peak profile analysis. *Journal of Theoretical and Applied Physics*, 8, pp.123-134.
- Bizarro, M., 2010. High photocatalytic activity of ZnO and ZnO:Al nanostructured films deposited by spray pyrolysis. *Applied Catalysis B: Environmental*, 97, pp.198-203.
- Blumel, S., Busse, H., Stolz, A. and Kampfer, P., 2001. *Xenophilus azovorans* gen. nov., sp. nov., a soil bacterium that is able to degrade azo dyes of the Orange II type. *International Journal of Systematic and Evolutionary Microbiology*, 51, pp.1831-1837.
- Campos Ventura-Camargo, B. and Marin-Morales, M., 2013. Azo dyes: Characterization and toxicity– A review. *Textiles and Light Industrial Science and Technology*, 2, pp.85-103.
- Chen, Q., Wang, F., Song, J. and Yuan, J., 2009. Photocatalytic degradation of alizarin yellow R using TiO₂ as catalyst: mechanistic and kinetic investigations. *Journal of Acta Scientiae Circumstantiae*, 29, pp.175-180.
- Chequer, F., de Oliveira, G., Anastacio Ferraz, E., Carvalho, J., Boldrin Zanoni, M. and de Oliveir, D., 2013. Textile dyes: Dyeing process and environmental impact. In: Gunay, M. ed. 2013. *Eco-Friendly Textile Dyeing and Finishing*, pp. 151-176.
- Coronado, J., Fresno, F., Hernandez-Alonso, M.D., Portela, R. eds., 2013. *Design of advanced photocatalytic materials for energy and environmental applications*. London: Springer, pp.15, 103-108.
- Dagdelen, S., Acemioğlu, B., Baran, E. and Koçer, O., 2014. Removal of remazol brilliant blue R from aqueous solution by pirina pretreated with nitric acid and commercial activated carbon. *Water, Air, & Soil Pollution*, 225, pp.1899-1913.
- Daghrir, R., Drogui, P. and Robert, D., 2013. Modified TiO₂ for environmental photocatalytic applications: A review. *Industrial & Engineering Chemistry Research*, pp. 3581-3599.
- Dalvand, A., Nabizadeh, R., Reza Ganjali, M., Khoobi, M., Nazmara, S. and Hossein Mahvi, A., 2016. Modeling of reactive blue 19 azo dye removal from colored textile wastewater using L-arginine-functionalized Fe₃O₄ nanoparticles: Optimization, reusability, kinetic and equilibrium studies. *Journal of Magnetism and Magnetic Materials*, 404, pp.179-189.
- Danwittayakul, S., Jaisai, M. and Dutta, J., 2015. Efficient solar photocatalytic degradation of textile wastewater using ZnO/ZTO composites. *Applied Catalysis B: Environmental*, 163, pp.1-8.
- Di Paola, A., García-López, E., Marci, G. and Palmisano, L., 2012. A survey of photocatalytic materials for environmental remediation. *Journal of Hazardous Materials*, 211-212, pp.3-29.

- Dindarloo, K., Jamali, H., Lakbala, P., Mahmoodi, H. and Kazemi, F., 2015. Feasibility of electrochemical oxidation process for treatment of saline wastewater. *Environmental Health Engineering and Management Journal*, 2, pp.129-134.
- Dridi-Dhaouadi, S. and Mhenni, M., 2014. Effect of dye auxiliaries on chemical oxygen demand and colour competitive removal from textile effluents using *Posidonia oceanica*. *Chemistry and Ecology*, 30, pp.579-588.
- Ghaedi, M., Ansari, A., Habibi, M. and Asghari, A., 2014. Removal of malachite green from aqueous solution by Zinc Oxide nanoparticle loaded on activated carbon: Kinetics and isotherm study. *Journal of Industrial and Engineering Chemistry*, 20, pp.17-28.
- Giri, P., Bhattacharyya, S., Chetia, B., Kumari, S., Singh, D. and Iyer, P., 2011. High-yield chemical synthesis of hexagonal ZnO nanoparticles and nanorods with excellent optical properties. *Journal of Nanoscience and Nanotechnology*, 12, pp.201-206.
- Gupta, V., Khamparia, S., Tyagi, I., Jaspal, D. and Malviya, A., 2015. Decolorization of mixture of dyes: A critical review. *Global Journal of Environmental Science Management*, 1, pp.71-94.
- Habib, M., Muslim, M., Shahadat, M., Islam, M., Ismail, I., Islam, T. and Mahmood, A., 2013. Photocatalytic decolorization of crystal violet in aqueous nano-ZnO suspension under visible light irradiation. *Journal of Nanostructure in Chemistry*, pp.70-79.
- Habibi, M. and Rahmati, M., 2015. The effect of operational parameters on the photocatalytic degradation of Congo red organic dye using ZnO–CdS core–shell nano-structure coated on glass by Doctor Blade method. *Spectrochimica Acta Part A: Molecular and Biomolecular Spectroscopy*, 137, pp.160-164.
- Hayat, K., Gondal, M., Khaled, M. and Ahmed, S., 2010. Kinetic study of laser-induced photocatalytic degradation of dye (Alizarin Yellow) from wastewater using nanostructured ZnO. *Journal of Environmental Science and Health, Part A*, 45, pp.1413-1420.
- Herrmann, J., 2010. Photocatalysis fundamentals revisited to avoid several misconceptions. *Applied Catalysis B: Environmental*, 99, pp.461-468.
- Hu, J. and Chen, H., 2015. preparation and activities of visible-light- driven BiVO₄ by doping Zn²⁺ via solid state method. *International Conference on Chemical, Material and Food Engineering*, 1, pp.241-244.
- Hung, Y., Wang, L. and Shamas, N. eds., 2012. *Handbook of environment and waste management*. Singapore: World Scientific Pub. Co., pp.930-933.
- Jabeen, M., Iqbal, M., Kumar, R., Ahmed, M. and Javed, M., 2014. Chemical synthesis of zinc oxide nanorods for enhanced hydrogen gas sensing. *Chinese Physics B*, 23, pp.018504.

- Jeyasubramanian, K., Hikku, G. and Sharma, R., 2015. Photo-catalytic degradation of methyl violet dye using zinc oxide nano particles prepared by a novel precipitation method and its anti-bacterial activities. *Journal of Water Process Engineering*, 8, pp.35-44.
- Jia, Z., Miao, J., Lu, H., Habibi, D., Zhang, W. and Zhang, L., 2016. Photocatalytic degradation and absorption kinetics of cibacron brilliant yellow 3G-P by nanosized ZnO catalyst under simulated solar light. *Journal of the Taiwan Institute of Chemical Engineers*, 60, pp.267-274.
- Johar, M., Afzal, R., Alazba, A. and Manzoor, U., 2015. Photocatalysis and band gap engineering using ZnO nanocomposites. *Advances in Materials Science and Engineering*, 2015, pp.1-22.
- Kamani, H., Bazrafshan, E., Ghozikali, M., Askari, M. and Ameri, R., 2015. Photocatalyst decolorization of C. I. Sulphur Red 14 from aqueous solution by UV irradiation in the presence of ZnO nanopowder. *Health Scope*, 4, pp.22248-22253.
- Karthik, V., Saravanan, K., Bharathi, P., Dharanya, V. and Meiaraj, C., 2014. An overview of treatments for the removal of textile dyes. *Journal of Chemical and Pharmaceutical Sciences*, 7, pp. 301-307.
- Kent, J. ed., 2012. *Handbook of industrial chemistry and biotechnology*. New York: Springer, pp.475-548.
- Khalid, A., Arshad, M. and Crowley, D., 2008. Decolorization of azo dyes by *Shewanella* sp. under saline conditions. *Applied Microbiology and Biotechnology*, 79, pp.1053-1059.
- Khalid, A., Kausar, F., Arshad, M., Mahmood, T. and Ahmed, I., 2012. Accelerated decolorization of reactive azo dyes under saline conditions by bacteria isolated from Arabian seawater sediment. *Applied Microbiology and Biotechnology*, 96, pp.1599-1606.
- Khan, R., Shamshi Hassan, M., Uthirakumar, P., Yun, J., Khil, M. and Lee, I., 2015. Facile synthesis of ZnO nanoglobules and its photocatalytic activity in the degradation of methyl orange dye under UV irradiation. *Materials Letters*, 152, pp.163-165.
- Khanlary, M., Vahedi, V. and Reyhani, A., 2012. Synthesis and characterization of ZnO nanowires by thermal oxidation of Zn thin films at various temperatures. *Molecules*, 17, pp.5021-5029.
- Klan, P. and Wirz, J. 2009. *Photochemistry of Organic Compounds- From Concepts to Practice*. Wiley, pp.423.
- Konstantinou, I. and Albanis, T., 2004. TiO₂-assisted photocatalytic degradation of azo dyes in aqueous solution: kinetic and mechanistic investigations. *Applied Catalysis B: Environmental*, 49, pp.1-14.

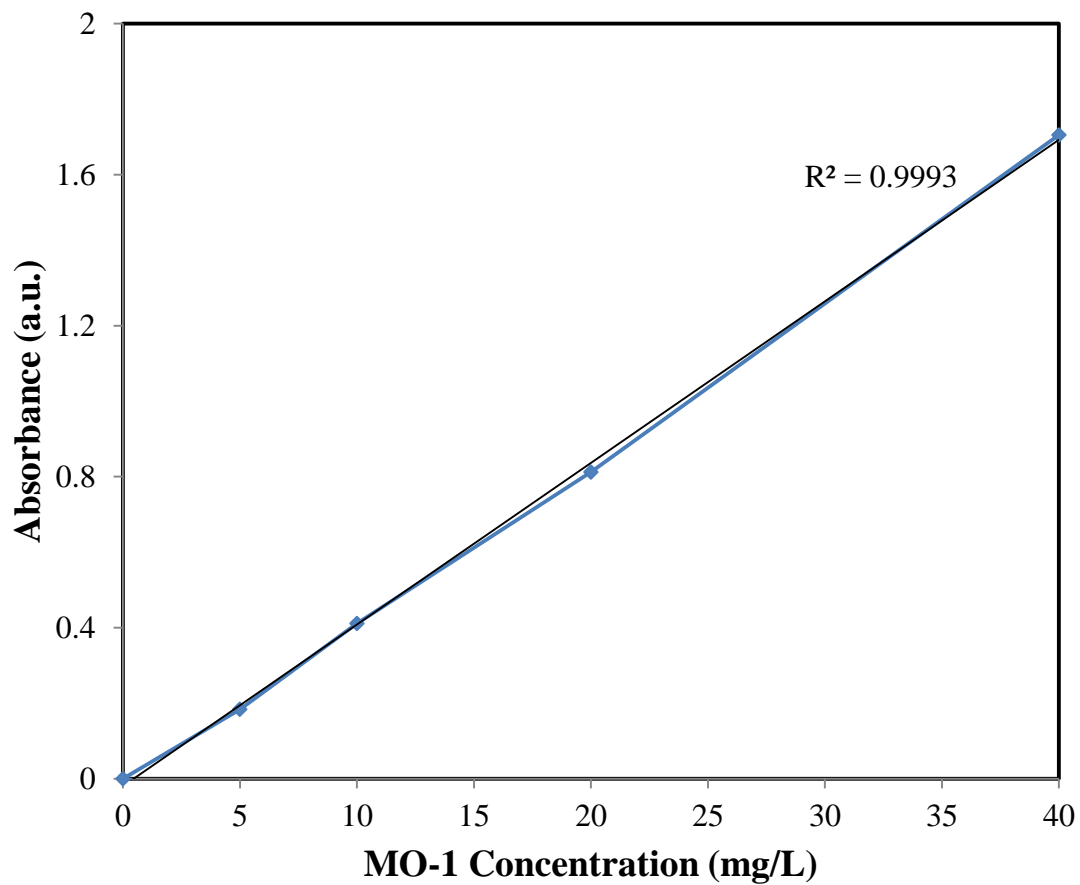
- Koprivanac, N. and Kusic, H., 2009. *Hazardous organic pollutants in colored wastewaters*. New York: Nova Science Publishers, pp. 2-4.
- Krishnakumar, B., Selvam, K., Velmurugan, R. and Swaminathan, M., 2010. Influence of operational parameters on photodegradation of Acid Black 1 with ZnO. *Desalination and Water Treatment*, 24, pp.132-139.
- Kulkarni, M. and Thakur, P., 2014. Photocatalytic degradation of real textile industrial effluent under UV light catalyzed by metal oxide nanoparticles. *Nepal Journal of Science and Technology*, 15, pp.105-110.
- Lam, S., Sin, J., Abdullah, A. and Mohamed, A., 2012. Degradation of wastewaters containing organic dyes photocatalysed by zinc oxide: a review. *Desalination and Water Treatment*, 41, pp.131-169.
- Lee, K., Lai, C., Ngai, K. and Juan, J. 2016, Recent developments of zinc oxide based photocatalyst in water treatment technology: A review. *Water Research*, 88, pp.428-448.
- Lin, J., Liu, X., Zhu, S., Liu, Y. and Chen, X., 2015. Anatase TiO₂ nanotube powder film with high crystallinity for enhanced photocatalytic performance. *Nanoscale Research Letter*, 10, pp.110-115.
- Liu, S., Min, Z., Hu, D. and Liu, Y., 2014. Synthesis of calcium doped TiO₂ nanomaterials and their visible light degradation property. *International Conference on Material and Environmental Engineering*, 1, pp.43-47.
- Malik, A. and Grohmann, E., 2012. *Environmental protection strategies for sustainable development*. Dordrecht: Springer, pp.111-162.
- Mezohegyi, G., van der Zee, F., Font, J., Fortuny, A. and Fabregat, A., 2012. Towards advanced aqueous dye removal processes: A short review on the versatile role of activated carbon. *Journal of Environmental Management*, 102, pp.148-164.
- Mobar, S., Kaushik, P. and Bhatnagar, P., 2015. Physiochemical comparison of textile effluent impacted and unimpacted agricultural soil of Jaipur city, India. *International Journal of Recent Scientific Research*, 6, pp. 3090- 3093.
- Mohanty, S., Dafale, N. and Rao, N. 2006, Microbial decolorization of reactive black-5 in a two-stage anaerobic-aerobic reactor using acclimatized activated textile sludge. *Biodegradation*, 17, pp.403-413.
- Muruganandham, M., Sobana, N. and Swaminathan, M., 2006. Solar assisted photocatalytic and photochemical degradation of Reactive Black 5. *Journal of Hazardous Materials*, 137, pp.1371-1376.
- Muthirulan, P., Meenakshisundaram, M. and Kannan, N., 2012. Beneficial role of ZnO photocatalyst supported with porous activated carbon for the mineralization of alizarin cyanin green dye in aqueous solution. *Journal of Advanced Research*, 4, pp.479-484.

- Ong, S., Min, O., Ho, L. and Wong, Y., 2012. Comparative study on photocatalytic degradation of mono azo dye acid orange 7 and methyl orange under solar light irradiation. *Water, Air, & Soil Pollution*, 223, pp.5483-5493.
- Pichat, P. ed., 2013. *Photocatalysis and water purification*. Weinheim: Wiley-VCH. pp. 3-4.
- Priyanka, and Srivastava, V., 2013. Photocatalytic oxidation of dye bearing wastewater by Iron doped Zinc Oxide. *Industrial & Engineering Chemistry Research*, 52, pp.17790-17799.
- Rana, S., Singh, P., Sharma, A., Carbonari, A. and Dogra, R., 2010. Synthesis and characterization of pure and doped ZnO nanoparticles. *Journal of Optoelectronics and Advanced Materials*, 12, pp.257 - 261.
- Ratna, and Padhi, B., 2012. Pollution due to synthetic dyes toxicity & carcinogenicity studies and remediation. *International Journal of Environmental Sciences*, 3, pp. 940-955.
- Rupa, A., Manikandan, D., Divakar, D., Revathi, S., Esther Leena Preethi, M., Shanti, K. and Sivakumar, T., 2007. Photocatalytic degradation of tatrazine dye using TiO₂ catalyst: Salt effect and kinetic studies. *Indian Journal of Chemical Technology*, 14, pp.71-78.
- Sakthivel, S., Neppolian, B., Shankar, M., Arabindoo, B., Palanichamy, M. and Murugesan, V. (2003). Solar photocatalytic degradation of azo dye: comparison of photocatalytic efficiency of ZnO and TiO₂. *Solar Energy Materials and Solar Cells*, 77, pp.65-82.
- Sanatgar-Delshade, E., Habibi-Yangjeh, A. and Khodadadi-Moghaddam, M., 2011. Hydrothermal low-temperature preparation and characterization of ZnO nanoparticles supported on natural zeolite as a highly efficient photocatalyst. *Monatshefte für Chemie - Chemical Monthly*, 142, pp.119-129.
- Sarayu, K. and Sandhya, S. 2012, Current technologies for biological treatment of textile wastewater—A review. *Appl Biochem Biotechnol*, 167, pp.645-661.
- Seddigi, Z., 2010. Removal of Alizarin Yellow dye from water using Zinc doped WO₃ catalyst. *Bulletin of Environmental Contamination Toxicology*, 84, pp.564-567.
- Sharma, S. and Sanghi, R. eds., 2012. *Advances in water treatment and pollution prevention*. Dordrecht: Springer. pp. 65-93.
- Sigma-Aldrich, 2016. *Mordant Orange 1*. [online] Sigma-Aldrich. Available at: <http://www.sigmaaldrich.com/catalog/product/sial/195073?lang=en®ion=MY> [Accessed 6 Apr. 2016].
- Singh, K. and Arora, S. 2011, removal of synthetic textile dyes From wastewaters: A critical review on present treatment technologies. *Critical Reviews in Environmental Science and Technology*, 41, pp.807-878.

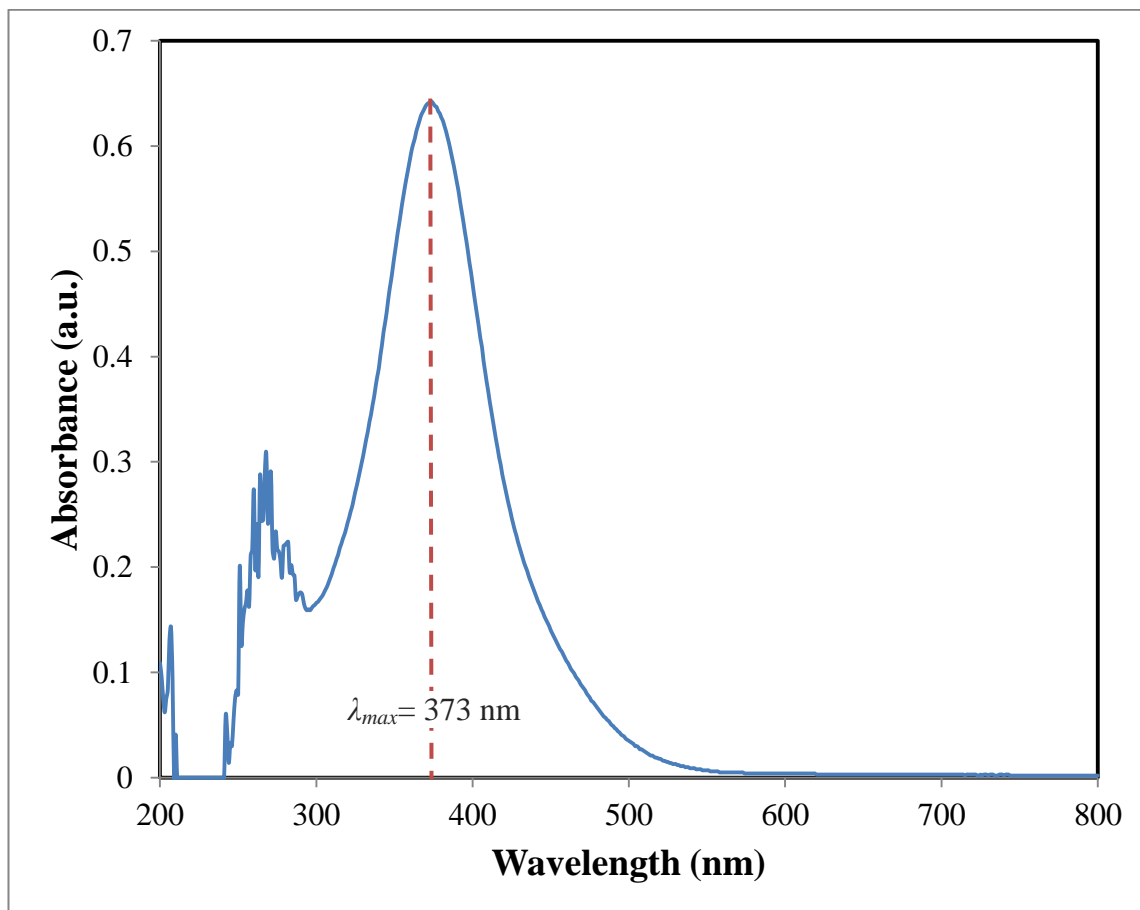
- Siuleiman, S., Kaneva, N., Bojinova, A., Papazova, K., Apostolov, A. and Dimitrov, D. 2014, Photodegradation of Orange II by ZnO and TiO₂ powders and nanowire ZnO and ZnO/TiO₂ thin films. *Colloids and Surfaces A: Physicochemical and Engineering Aspects*, 460, pp.408-413.
- Sobana, N. and Swaminathan, M. 2007, The effect of operational parameters on the photocatalytic degradation of acid red 18 by ZnO. *Separation and Purification Technology*, 56, pp.101-107.
- Sobana, N., Krishnakumar, B. and Swaminathan, M. 2013, Synergism and effect of operational parameters on solar photocatalytic degradation of an azo dye (Direct Yellow 4) using activated carbon-loaded Zinc Oxide. *Materials Science in Semiconductor Processing*, 16, pp.1046-1051
- Soltani, R., Shams Khoramabadi, G., Godini, H. and Noorimotlagh, Z., 2015. The application of ZnO/SiO₂ nanocomposite for the photocatalytic degradation of a textile dye in aqueous solutions in comparison with pure ZnO nanoparticles. *Desalination and Water Treatment*, 56, pp.2551-2558.
- Tan, L., He, M., Song, L., Fu, X. and Shi, S., 2015. Aerobic decolorization, degradation and detoxification of azo dyes by a newly isolated salt-tolerant yeast *Scheffersomyces spartinae* TLHS-SF1. *Bioresource Technology*, 203, pp.287-294.
- Tiwari, D., Lalhriatpuia, C., Lalmunsiam, Lee, S. and Kong, S., 2015. Efficient application of nano-TiO₂ thin films in the photocatalytic removal of alizarin yellow from aqueous solutions. *Applied Surface Science*, 353, pp.275-283.
- Turhan, K., Durukan, I., Ozturkcan, S. and Turgut, Z., 2012. Decolorization of textile basic dye in aqueous solution by ozone. *Dyes and Pigments*, 92, pp.897-901.
- Vacchi, F., Albuquerque, A., Vendemiatti, J., Morales, D., Ormond, A., Freeman, H., Zocolo, G., Zanoni, M. and Umbuzeiro, G., 2013. Chlorine disinfection of dye wastewater: Implications for a commercial azo dye mixture. *Science of The Total Environment*, 442, pp.302-309.
- Vasanthkumar, K., Porkodi, K. and Selvaganapathi, A., 2007. Constrain in solving Langmuir–Hinshelwood kinetic expression for the photocatalytic degradation of Auramine O aqueous solutions by ZnO catalyst. *Dyes and Pigments*, 75, pp.246-249.
- Wang, Y., Lu, K. and Feng, C., 2013. Influence of inorganic anions and organic additives on photocatalytic degradation of methyl orange with supported polyoxometalates as photocatalyst. *Journal of Rare Earths*, 31, pp.360-365.
- Wong, K., 2016. *Comparative study on photocatalytic removal of Rhodamine B by Zinc Oxide and Titanium Dioxide nanoparticles*. Universiti Tunku Abdul Rahman.
- Yamjala, K., Nainar, M. and Ramiseti, N., 2015. Methods for the analysis of azo dyes employed in food industry – A review. *Food Chemistry*, 192, pp.813-824.

- Yao, L., Zhang, L., Wang, R., Chou, S. and Dong, Z., 2016. A new integrated approach for dye removal from wastewater by polyoxometalates functionalized membranes. *Journal of Hazardous Materials*, 301, pp.462-470.
- Yin, H., Coleman, V., Casey, P., Angel, B., Catchpoole, H., Waddington, L. and McCall, M., 2015. A comparative study of the physical and chemical properties of nano-sized ZnO particles from multiple batches of three commercial products. *Journal of Nanoparticle Research*, 17, pp.96-114.
- Yu, C., Yang, K., Shu, Q., Yu, J., Cao, F., Li, X. and Zhou, X., 2012. Preparation, characterization and photocatalytic performance of Mo-doped ZnO photocatalysts. *Science China*, 55, pp.1802–1810.
- Yu, L., Zhang, X., Tang, Q., Li, J., Xie, T., Liu, C., Cao, M., Zhang, R., Wang, S., Hu, J., Qiao, W., Li, W. and Ruan, H., 2011. Decolorization characteristics of a newly isolated salt-tolerant *Bacillus* sp. strain and its application for azo dye-containing wastewater in immobilized form. *Appl Microbiol Biotechnol*, 99, pp.9277-9287.
- Yuan, R., Ramjaun, S., Wang, Z. and Liu, J., 2012. Photocatalytic degradation and chlorination of azo dye in saline wastewater: Kinetics and AOX formation. *Chemical Engineering Journal*, 192, pp.171-178.
- Zaharia, C. and Suteu, D., 2012. Textile organic dyes – characteristics, polluting effects and separation/elimination procedures from industrial effluents – A critical overview. *Organic Pollutants Ten Years After the Stockholm Convention - Environmental and Analytical Update*, pp. 55-86.

APPENDICES



Appendix I: Mordant Orange-1 (MO-1) Calibration Curve



Appendix II: Mordant Orange-1 (MO-1) UV-Vis Absorption Spectra.